THE ROLE MAPK1 PLAYS IN DRP1 ACTIVATION LEADING TO MITOCHONDRIAL DYSFUNCTION IN HUNTINGTON'S DISEASE

by

ANNE J.T. ROE

Submitted in partial fulfillment of the requirements for the degree of

Master of Science

Thesis Advisor: Xin Qi, Ph.D.

Department of Physiology and Biophysics

Medical Physiology

CASE WESTERN RESERVE UNIVERSITY

May 2016

CASE WESTERN RESERVE UNIVERSITY

SCHOOL OF GRADUATE STUDIES

We hereby approve the thesis of

Anne J.T. Roe

Candidate for the degree of Master of Science.*

Committee Chair

William Schilling, Ph.D.

Committee Member

Xin Qi, Ph.D.

Committee Member

George Dubyak, Ph.D.

Committee Member

Joseph LaManna, Ph.D.

Committee Member

Charles Hoppel, M.D.

Date of Defense

Friday, March 18, 2016

*We also certify that written approval has been obtained for any proprietary material contained therein.

DEDICATION

To my parents, Stephen and Adrienne, whose encouragement, understanding, and love everyday reminds me to never stop following my dreams and working hard for what I am passionate about.

To my sisters, Sarah and Rebecca, who have made me who I am; we are on this journey through life together, no matter the space between us.

To my friends who remind me to, and help me to, enjoy life along the way.

"Imagination is more important than knowledge"- Albert Einstein

TABLE OF CONTENTS

List of Figures.....6

Acknowledgements.....8

List of Abbreviations.....9

Abstract.....10

Chapter I: Introduction.....11

1.1 Huntington's disease.....11

1.2 Mitochondrial dysfunction in neurodegeneration.....13

1.3 Dynamin-related protein 1.....17

1.4 Mitogen-activated protein kinase 1 and mitochondrial dysfunction.....18

1.5 Hypothesis and specific aims of project.....20

Chapter II: Results and Discussion.....22

2.1 Drp1 is phosphorylated in HD cell culture models.....22

2.2 In vitro phosphorylation results.....25

2.3 Identifying the site of Drp1 phosphorylation in HD and the role MAPK1 inhibition has on cell signaling in HD.....29

2.4 The effect of MAPK1 inhibition on mitochondrial morphology, mitochondrial function, and neuronal cell death in HD.....33

Chapter III: Materials and Methods.....45

Chapter IV: Future Direction.....54

4.1 Additional experiments.....54

4.2 The mechanism underlying Drp1 activation by MAPK1 in HD.....56

4.3 Additional HD models.....57

4.4 MAPK1 and mutant huntingtin.....59

Appendix I: Supplemental Figures- Chromatograms and Spectra.....61

References.....69

LIST OF FIGURES

Table 1. Serine residues phosphorylated by MAPK1 and their domain.....29

Table 2. List of antibodies.....50

Figure 1. The human brain, showing the impact of HD, on the basal ganglia.....12

Figure 2. Functional alterations in HD mitochondria.....14

Figure 3. Modeling of predicted human Drp1 structure (isoform 3).....17

Figure 4. Drp1 interactome in striatal neurons derived from HD patient-iPS cells.....20

Figure 5. Serine/threonine phosphorylation of Drp1 in HD.....23

Figure 6. The effect of kinase inhibitors on overall serine/threonine phosphorylation of Drp1 in HD.....24

Figure 7. *In vitro* phosphorylation assay of Drp1 and MAPK1.....26

Figure 8. SDS-PAGE gel with Coomassie blue staining for mass spectrometry analysis.....27

Figure 9. Relative abundance of Drp1 phosphorylation sites targeted by MAPK1.....28

Figure 10. Ser616 and Ser637 phosphorylation of Drp1 in HD and the effect of MAPK1 inhibition.....30

Figure 11. Drp1 oligomerization in HD and the effect of MAPK1 inhibition.....33

Figure 12. The effect MAPK1 inhibition has on mitochondrial fragmentation in HD.....35

Figure 13. The effect MAPK1 inhibition has on mitochondrial membrane potential in HD.....37

Figure 14. The effect MAPK1 inhibition has on mitochondrial ROS production in HD....38

Figure 15. The effect MAPK1 inhibition has on neuronal cell death in HD....40

Figure 16. The role Drp1 Ser616 plays in mitochondrial fragmentation in HD....42

Figure 17. Summary of Drp1 activation by MAPK1 leading to the mitochondrial fragmentation observed in HD....44

Figure 18. Schematic of U0126 inhibition of Drp1 phosphorylation by ERK2 (MAPK1)....48

Figure 19. The role mtHtt plays in MAPK1 and Drp1 activation in HD....60

Figure A1. HPLC chromatogram of trypsin digest of Drp1 phosphorylated by MAPK1....61

Figure A2. HPLC chromatogram of chymotrypsin digest of Drp1 phosphorylated by MAPK1....62

Figure A3. CID mass spectrum of phosphopeptide identifying S126....63

Figure A4. CID mass spectrum of phosphopeptide identifying S248....64

Figure A5. CID mass spectrum of phosphopeptide identifying S275....65

Figure A6. CID mass spectrum of phosphopeptide identifying S529....66

Figure A7. CID mass spectrum of phosphopeptide identifying S590....67

Figure A8. CID mass spectrum of phosphopeptide identifying S611....68

ACKNOWLEDGEMENTS

I would like to thank the Qi research group: Xing Guo, Yuanyuan Zhao, Di Hu, and Xiaoyan Sun for their support throughout my thesis. I would like to thank Xing Guo specifically for helping to train me in techniques and analysis I was unfamiliar with, and for taking the time from his busy schedule to answer my questions and listen to my ideas. I would also like to thank Dr. Xin Qi for allowing me to conduct research in her group and providing me with the facilities and resources necessary to complete this project in such a short period of time.

To my graduate thesis committee: Dr. George Dubyak, Dr. Joseph LaManna, Dr. Charles Hoppel, and my committee chair Dr. William Schilling. Thank you for your time, patience, and input throughout my project. Your expertise and questions challenged me to get a deeper and more thorough understanding of my project. I would like to specifically thank Dr. Hoppel for helping to expand my knowledge in mitochondrial physiology by including me in Journal Club, the Bioenergetics review sessions, and the Data Conferences for the mitochondria group at CWRU.

I would also like to thank Dr. Thomas Nosek, Dr. Andrea Romani, and the members of the M.S. in Medical Physiology Administration Committee for accepting me into this program and allowing me to conduct unique research with a neurodegenerative disease. I would also like to thank my advisors, Dr. Joseph LaManna, and Dr. Corey Smith, for preparing me for the thesis track in my first year.

Finally, a special thank you to Dr. Martina Wiedau-Pazos, whose invaluable undergraduate mentoring has given me the experience I need to succeed.

LIST OF ABBREVIATIONS

DMEM	Dulbecco's modified Eagle's medium
DMSO	dimethyl sulfoxide
Drp1	dynamin-related protein 1
DTT	dithiothreitol
ERK2	extracellular signal-regulated kinase 2
HD	Huntington's disease
HeLa	Henrietta Lacks
IP	immunoprecipitation
iPS	induced pluripotent stem cells
KO	knockout
LDH	lactate dehydrogenase
MEK1/2	mitogen-activated protein kinase kinase 1/2
MAPK1	mitogen-activated protein kinase 1
mtHtt	mutant huntingtin protein
PBS	phosphate-buffered saline
PKCδ	protein kinase Cδ
ROS	reactive oxygen species
SDS-PAGE	sodium dodecyl sulfate-polyacrylamide gel electrophoresis
siRNA	short interfering RNA

The Role MAPK1 Plays in Drp1 Activation Leading to Mitochondrial Dysfunction in Huntington's Disease

Abstract

by

ANNE J.T. ROE

Huntington's disease (HD) is an incurable neurodegenerative disease with autosomal dominant inheritance caused by expanded CAG repeats in the *huntingtin gene* that confers a toxic gain-of-function on mutant huntingtin (mtHtt) protein. Mitochondrial dysfunction is a major cytopathology in HD. However, the molecular mechanisms by which mtHtt affect mitochondrial function remains elusive. This project explores the role MAPK1 plays in the over-activation of Drp1, the mitochondrial fission protein, which leads to the mitochondrial dysfunction and neurodegeneration seen in HD. Hdh striatal cells, treated with U0126, a potent inhibitor of MEK1/2, showed a decrease in mitochondrial fragmentation, and restored mitochondrial function. We show MAPK1 binding to and phosphorylating Drp1 at Ser616 in HD, as well as U0126 treatment abolishing this phosphorylation. A phosphorylation-deficient mutant of Drp1, S616A, also corrected the mitochondrial fragmentation associated with HD. This study suggests that MAPK1 activation of the mitochondrial fission machinery leads to the aberrant mitochondrial dysfunction and neurodegeneration seen in HD; and that inhibition of Drp1-mediated excessive mitochondrial fission can be used as a treatment for HD.

CHAPTER I: INTRODUCTION

1.1 Huntington's disease

Huntington's disease (HD) is an incurable neurodegenerative disease with a prevalence of 5.70 per 100,000 in North America, Europe, and Australia.[1] The disease was named after George Huntington, who described the condition in 1872 in *The Medical and Surgical Reporter.*[2] The disease's main clinical feature, chorea, was first described by Charles Oscar Waters in 1841 as a "spasmodic action of all the voluntary muscles of the system."[3] The pathology of HD involves neurodegeneration of the corpus striatum (**Figure 1**), which accounts for the motor, psychiatric, and cognitive features of the disease and was first described by Meynert in 1877.[4]

The gene *huntingtin* (*HTT*) was discovered in 1993 by The Huntington's Disease Collaborative Research Group, and encodes an ubiquitously expressed 350kDa protein called huntingtin.[5] The mutation causes an abnormal expansion of the trinucleotide repeat CAG, within the coding sequence of the gene, resulting in a mutant form of the protein with an expanded polyglutamine tract. Pathogenic gain-of-function results when the length of this tract reaches 36 or more repeats.[6,7] Of note, expanded CAG repeats alone can be toxic, producing polyglutamine peptides known to cause neurodegeneration.[8,9]

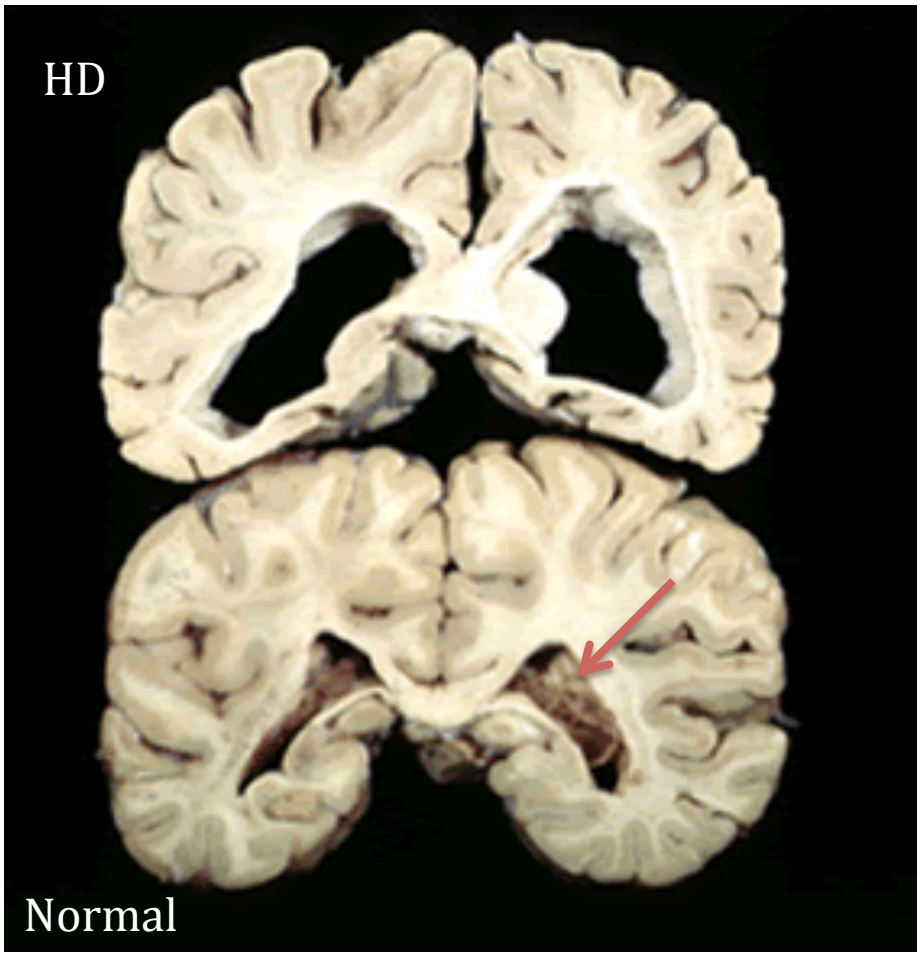

Figure 1. The human brain, showing the impact of HD, on the basal ganglia. (Top) a person with HD, where the loss of the striatum causes an enlargement of the ventricles; compared to (bottom) a normal brain (red arrow pointing to the basal ganglia). http://kobiljak.msu.edu

1.1.1 Wild-type huntingtin versus mutant huntingtin

Wild-type huntingtin is mainly a cytosolic protein, although some have reported that the first 17/18 amino acids of the N-terminal of huntingtin plays a role in targeting huntingtin to the following membrane-bound organelles: mitochondria, endocytic and autophagic vesicles, the Golgi apparatus, and the endoplasmic

reticulum (ER).[10,11] Huntingtin has been shown to be essential for normal embryonic development[12,13], neuronal survival and testicular viability[14], as well as protecting against apoptotic insults.[15-17]

Proteolysis of mutant huntingtin (mtHtt) plays an important role in the toxicity of the protein, as groups have shown that the N-terminal fragments are more toxic than the full-length mtHtt protein.[18,19] This increase in toxicity can be explained by the nuclear localization of mtHtt N-terminal fragments,[20,21] allowing the polyglutamine tract to interact with transcription factors, thus altering transcription.[22] Mutant huntingtin protein aggregates into intranuclear and intracytoplasmic inclusions and are a main pathological feature of HD. However, while some groups have reported a correlation between these aggregates and cellular toxicity,[23,24] others have reported a protective role for these aggregates.[25,26]

1.2 Mitochondrial dysfunction in neurodegeneration

Mitochondrial dysfunction is a hallmark with many neurodegenerative diseases and has therefore become a main hypothesis to explain the cellular mechanism of these diseases.[27-29] Mitochondria are vital for energy production, and neurons, who have high electrical activity and cannot use glycolysis as a source of ATP, are extremely dependent on mitochondria for the metabolic demand of regulating Ca^{2+}, maintaining resting membrane potential, allowing for axonal and

dendritic transport, and allowing for the release and re-uptake of neurotransmitters.[30,31]

1.2.1 Mitochondrial dysfunction in HD

Seong et al. 2005 has reported an inverse relationship between CAG repeats and mitochondrial ATP production: as repeat number increases, ATP/ADP ratio decreases.[32] The mitochondria also have a reduced membrane potential and a higher susceptibility to NMDA-mediated Ca^{2+} influx leading to excitotoxicity.[33,34] There are currently five theories (summarized in **Figure 2**)[35] as to how mtHtt causes mitochondrial dysfunction in HD.

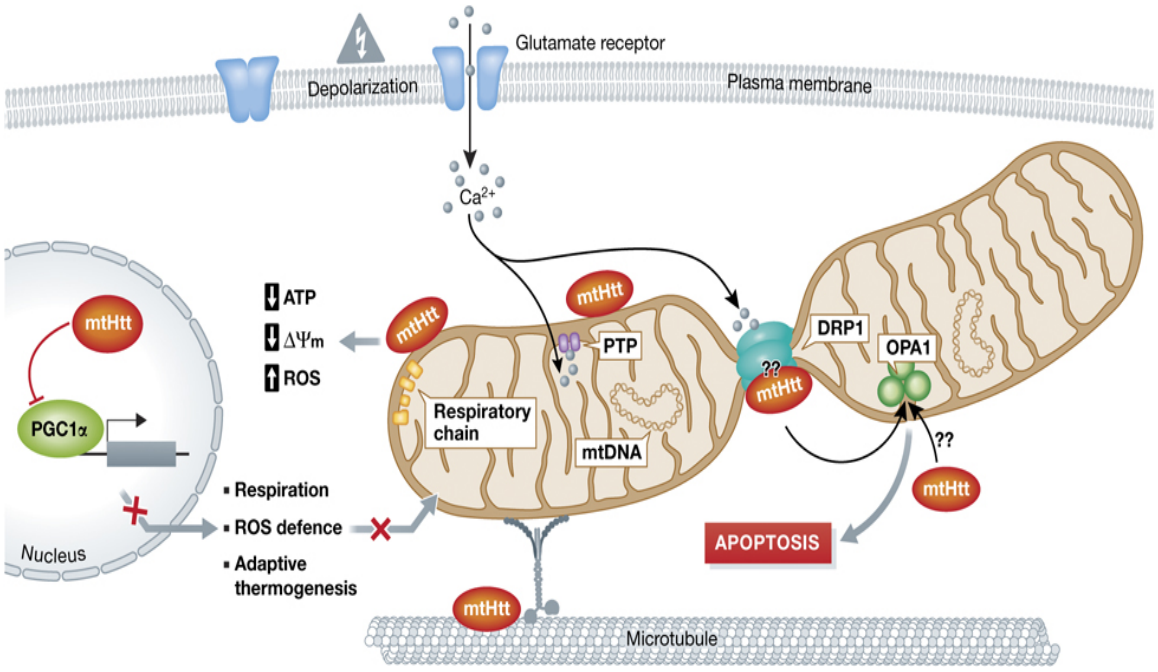

Figure 2. Functional alterations in HD mitochondria. mtHtt is mutant huntingtin.[35]

As discussed earlier, mtHtt N-terminal fragments can enter the nucleus and

alter gene transcription. PGC1α (peroxisome proliferator-activated receptor-γ coactivator 1α) is a transcriptional coactivator and a master regulator of energy homeostasis, which has been shown to be involved in adaptive thermogenesis and ROS (reactive oxygen species) defense, as well as enhance transcription of respiratory complexes and increase mtDNA (mitochondrial DNA). PGC1α levels and activity have been shown to be lower than normal in HD patient brain and muscle samples, as well as in transgenic mice models.[36-38] The hypothesis is that mtHtt binds to and inhibits PGC1α, impairing mitochondrial function, and leading to the neurodegeneration seen in HD.

Mutant huntingtin has been shown to interact directly with mitochondria regulating their calcium handling capacity.[39] The decreased ATP/ADP ratio over-activates NMDA receptors, allowing a greater influx of Ca^{2+} into the neurons. Another role for mitochondria is to store cellular Ca^{2+}, but an excess of Ca^{2+} in the mitochondrial matrix opens the permeability transition pore (PTP), which is a high conductance unselective channel in the inner mitochondrial membrane. The opening of the PTP will cause mitochondrial swelling that leads to the release of proapoptotic factors.[40]

A third hypothesis for mitochondrial dysfunction in HD involves the direct or indirect impairment of electron transport chain (ETC) complexes and tricarboxylic acid (TCA) cycle enzymes by mtHtt. ETC complexes II, III, and IV have been shown to have a reduced activity in advanced stages of HD.[41,42] This impairment of the respiratory chain leads to the decrease in ATP, decrease in mitochondrial membrane potential, and increase in ROS seen in HD.

The impaired trafficking of organelles is the fourth hypothesis for mitochondrial dysfunction in HD. As discussed earlier, mtHtt forms aggregates, which can physically impair the passage of mitochondria along neuronal processes. Furthermore, mtHtt binds to its partner huntingtin-associated protein (HAP1) to regulate transport through interactions with kinesin and dynein.[43]

Changes in mitochondrial morphology have been associated with ATP production[44], ROS generation[45], movement[46], and apoptosis[47]. Mitochondrial morphology is maintained through a balance of fusion and fission events that are regulated by GTPases to maintain shape, number, and functionality. Optic atrophy 1 (Opa1) on the inner mitochondrial membrane and mitofusions 1 and 2 (Mfn1 and Mfn2) on the outer mitochondrial membrane regulate mitochondrial fusion; whereas, dynamin-related protein 1 (Drp1) in the cytosol regulates mitochondrial fission through its molecular adaptors, namely Fis1, Mff, and MiD49/51, on the outer mitochondrial membrane. The release of cytochrome c, a proapoptotic factor, requires fragmentation and cristae remodeling[48,49] and the inhibition of Drp1 has been shown to prevent mitochondrial fragmentation, the release of cytochrome c, and cell death.[50] Thus, the last hypothesis states that mtHtt either directly or indirectly over-activates Drp1, resulting in mitochondrial fragmentation. However, it is also possible that mtHtt disturbs the balance of fusion and fission events by inhibiting mitochondrial fusion, leading to the excessive mitochondrial fission seen in HD.

1.3 Dynamin-related protein 1

Dynamin-related protein 1 (Drp1, **Figure 3**)[51] is a cytosolic GTPase that regulates the mitochondrial fission events, which is important for mitochondrial renewal, proliferation, and redistribution.[31,52] Drp1 can undergo post-translational modification, including phosphorylation, ubiquitination, and sumoylation that can modify its GTPase activity, its cellular location, and its oligomerization. Upon activation Drp1 will translocate to the mitochondria, oligomerize, and bind to its molecular adaptor at constriction sites, leading to division of the mitochondria. Excessive mitochondrial fission causes mitochondrial fragmentation, which leads to permeabilization of the outer mitochondrial membrane, ATP depletion, increase of ROS, and release of apoptotic factors.[51]

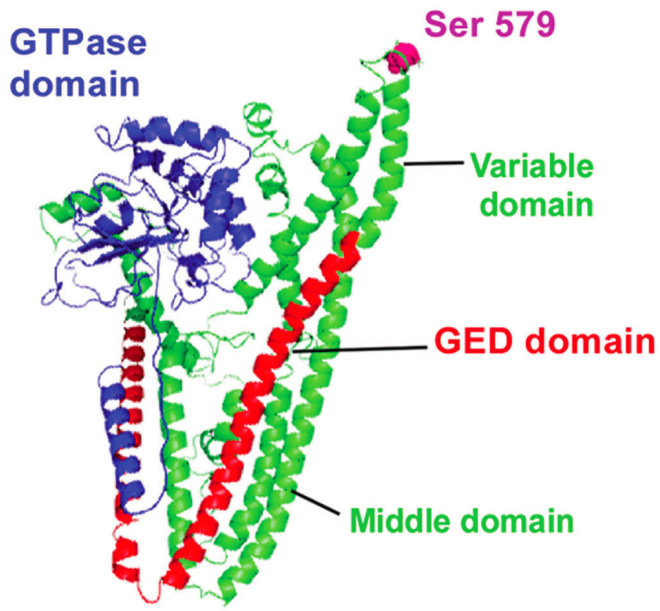

Figure 3. Modeling of predicted human Drp1 structure (isoform 3). Blue: GTPase domain; green: middle domain and variable domain; red: GTPase effector domain (GED). *Note: Ser579 in Drp1 isoform 3 corresponds to Ser616 in Drp1 isoform 1.[51]

1.3.1 Drp1 has been implicated in neurodegeneration

Phosphorylation of Drp1 by different serine/threonine kinases in normal physiology and pathophysiology has different outcomes on the GTPase activity of the protein. There are two main serine residues on Drp1 that regulate its GTPase activity: Ser616 and Ser637 (isoform 1). Ser616 is phosphorylated by cyclin-dependent kinase 1 (Cdk1) in mitosis, where fission and proliferation of the mitochondria is required for proper distribution of the mitochondria between the two daughter cells.[53] Conversely, when Ser616 is phosphorylated by protein kinase Cδ (PKDδ) under oxidative stress conditions the mitochondrial fragmentation leads to impaired mitochondrial function.[51] Ser637 phosphorylation by protein kinase A (PKA) has been shown to decrease its GTPase activity, protecting the mitochondria, and leading to cell survival.[54,55] However, dephosphorylation of Ser637 by the phosphatase calcineurin removes this protection of the mitochondria, and the hyper-fission leads to apoptosis.[55] Furthermore, the Gly2019Ser mutation in the LRRK2 kinase in Parkinson's disease has been shown to phosphorylate Drp1 at Thr595, and the resulting excessive fission damages the mitochondria leading to cell death.[56]

1.4 Mitogen-activated protein kinase 1 and mitochondrial dysfunction

Mitogen-activated protein kinase 1 (MAPK1/ERK2) is a serine/threonine

kinase and is a component of the MAP kinase signal transduction pathway. This pathway when activated has many cellular effects including regulation of cell growth, survival, and differentiation. MAPK1 has been implicated in mitochondrial dysfunction that leads to apoptosis[57] and cancer.[58,59] Pyakurel et al. 2015 has shown that MAPK1 phosphorylates the mitochondrial fusion protein Mfn1, inhibiting mitochondrial fusion, leading to mitochondrial fragmentation, mitochondrial permeabilization, and cellular apoptosis.[57] Serasinghe et al., 2015 found that Ser616 phosphorylation of Drp1 by MAPK1 activated its GTPase activity and was required for Ras-induced cellular transformation, by increasing mitochondrial fission and dysfunction.[58] They also noted that MAPK1 did not phosphorylate Drp1 at Ser637, which would have decreased its GTPase activity. Kashatus et al., 2015 noted that Ser616 phosphorylation of Drp1 by MAPK1 leads to mitochondrial fission and tumor growth.[59]

1.4.1 MAPK1's role in mitochondrial dysfunction in HD

Our lab has recently analyzed the interactome of Drp1 in neurons derived from HD-patient iPS (induced pluripotent stem) cells. As shown in **Figure 4** HD-patient iPS cells were differentiated into neuronal cells, from which total lysates were collected. Drp1 was then immunoprecipitated with anti-Drp1 antibodies and analyzed via mass spectrometry. The protein ID identified MAPK1 as the leading kinase that binds to Drp1 in HD. A few previously mentioned studies have shown that post-translational modification, especially phosphorylation, of Drp1 regulates

its GTPase activity. Moreover, given recent studies showing that MAPK1 phosphorylates Drp1 in cancer, there is promise for MAPK1 and Drp1 interaction in HD models. This would help us better understand the molecular mechanism by which mtHtt leads to the mitochondrial fragmentation and dysfunction seen in HD.

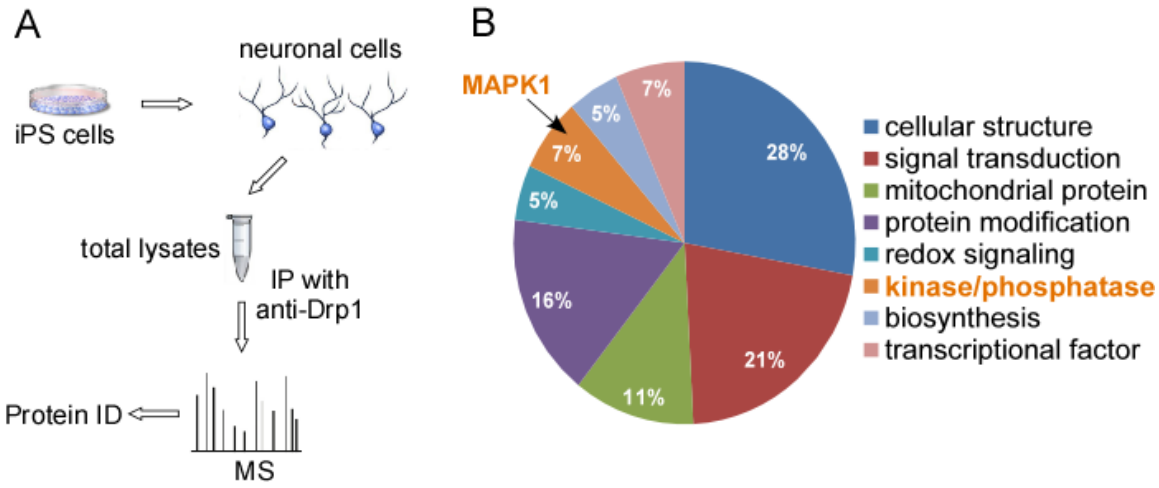

Figure 4. Drp1 interactome in striatal neurons derived from HD patient-iPS cells **(A)** Proteomic analysis of Drp1 interactome **(B)** Molecular and Cellular Function of Drp1 interactome.

1.5 Hypothesis and specific aims of project

I **hypothesize** that MAPK1 hyper-activates Drp1, via phosphorylation, in HD causing mitochondrial fragmentation, mitochondrial dysfunction, and neuronal cell death. The following specific aims will be investigated:

Aim #1: To determine whether MAPK1 phosphorylates Drp1 at serine sites Ser616 or Ser637

- Using Hdh mouse striatal cells

- In the presence and absence of the MEK1/2 inhibitor, U0126

Aim #2: To evaluate whether MAPK1 phosphorylates Drp1 at any other serine/threonine sites.

- Using an *in vitro* phosphorylation assay with human recombinant Drp1 and MAPK1 analyzed via mass spectrometry

Aim #3: To determine whether Drp1 phosphorylation by MAPK1 affects mitochondrial morphology and function as well as neuronal viability in models of HD.

- Using Hdh mouse striatal cells
- In the presence and absence of the MEK1/2 inhibitor, U0126
- Also, using a phosphorylation-deficient mutant of Drp1, S616A

CHAPTER II: RESULTS AND DISCUSSION

2.1 Drp1 is phosphorylated in HD cell culture models

Drp1 has an increased serine/threonine phosphorylation level, and more MAPK1 binds to Drp1, in models of HD compared to wild-type models

Our lab[60] and others[61] have shown mitochondrial fragmentation in models of HD. To determine the overall serine/threonine phosphorylation level of Drp1 in cell culture models of HD, total lysates were harvested from both Hdh mouse striatal cells and HeLa human epithelial cells. Drp1 was imunoprecipitated and then the membrane was probed with anti-p-S/T (phosphorylation at serine/threonine sites), anti-MAPK1, and anti-Drp1. Western blot analysis shows that the overall serine/threonine phosphorylation level of Drp1 is higher in both the mutant HdhQ111 striatal cells (**Figure 5A, B**) and in the mutant HeLa cells expressing full-length mtHtt with Q73 (**Figure 5E, F**) compared to the wild-type cells. The western blot analysis also shows that with immunoprecipitation of Drp1 there is more MAPK1 interacting with Drp1 in the mutant HdhQ111 striatal cells (**Figure 5C, D**) and in the mutant HeLa cells with Q73 (**Figure 5G, H**) compared to the wild-type cells. The increase in Drp1 serine/threonine phosphorylation in cell culture models of HD compared to wild-type models suggests that excessive mitochondrial fission plays a role in the pathogenesis of HD. These initial results also suggest that MAPK1 binds to Drp1 in cell culture models of HD.

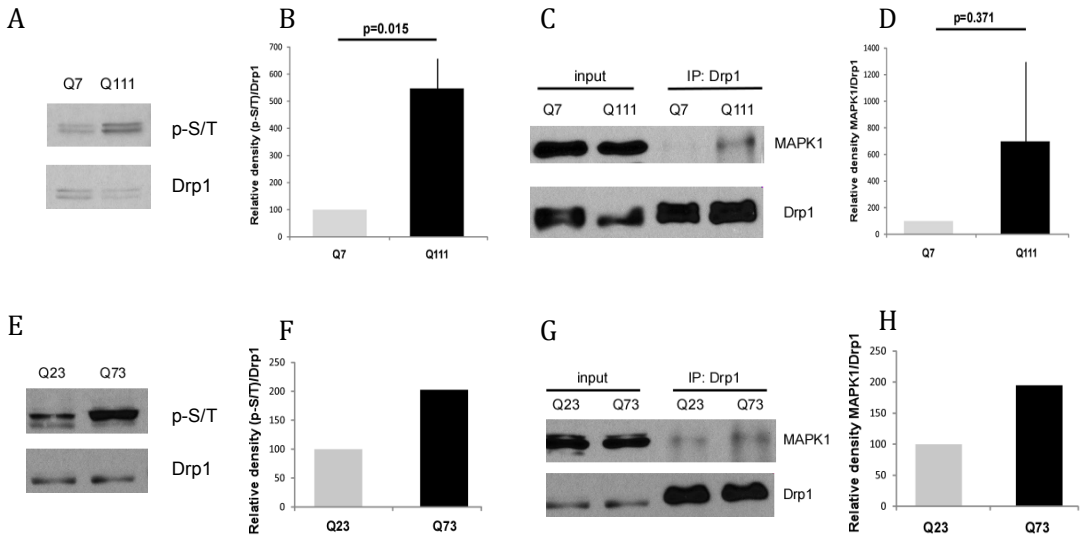

Figure 5. Serine/threonine phosphorylation of Drp1 in HD. **(A-B)** Serine/threonine phosphorylation of Drp1 from input samples from Hdh striatal cells. Phosphorylation level was quantified compared to total Drp1 level, n=3 **(C-D)** MAPK1 from IP samples from Hdh striatal cells. MAPK1 level was quantified compared to total Drp1 level, n=3 **(E-F)** Serine/threonine phosphorylation of Drp1 from input samples from HeLa epithelial cells. Phosphorylation level was quantified compared to total Drp1 level, n=1 **(G-H)** MAPK1 from IP samples from HeLa epithelial cells. MAPK1 level was quantified compared to total Drp1 level, n=1

The serine/threonine phosphorylation of Drp1 that is observed in models of HD is decreased by inhibition of MAPK1 but not inhibition of PKCδ

Qi et al., 2011 showed that the phosphorylation of Drp1 at Ser616 was decreased with δV1-1, a PKCδ inhibitor, when cultured SH-SY5Y cells were exposed to oxidative stress.[51] In order to form a greater understanding of the serine/threonine phosphorylation of Drp1 that is observed in cell culture models of HD, the cell culture models were treated with kinase inhibitors. The Hdh striatal cells and the HeLa epithelial cells were treated with DMSO (control), 10μM PD98059

(MEK1/2 inhibitor), or 1μM δV1-1 for one hour. Total lysates were harvested, Drp1 immunoprecipitated, and then the membrane was probed with anti-p-S/T, anti-MAPK1, and anti-Drp1. Western blot analysis shows the overall serine/threonine phosphorylation of Drp1 decreased with PD98059 in the mutant HdhQ111 striatal cells (**Figure 6A, B**) and in the mutant HeLa cells with Q73 (**Figure 6D, E**). Western blot analysis also shows that there is no change in overall serine/threonine phosphorylation of Drp1 with δV1-1 in the mutant HdhQ111 striatal cells (**Figure 6A, C**) and in the mutant HeLa cells with Q73 (**Figure 6D, F**). These results suggest that MAPK1, and not PKCδ, plays a role in Drp1 phosphorylation in cell culture models of HD.

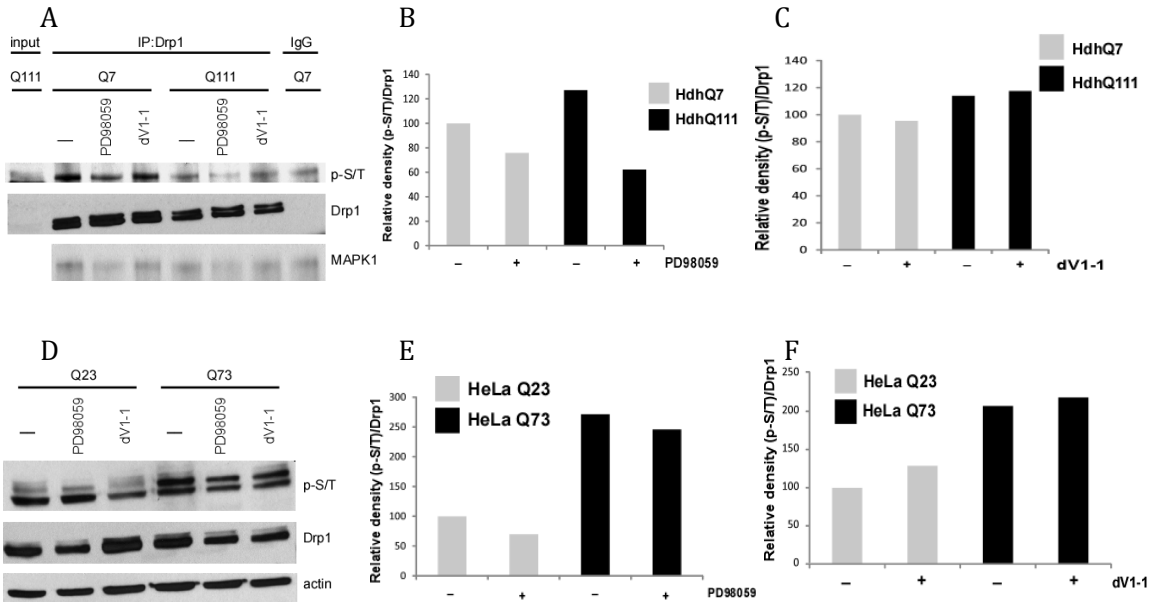

Figure 6. The effect of kinase inhibitors on overall serine/threonine phosphorylation of Drp1 in HD. **(A-C)** Serine/threonine phosphorylation of Drp1 from IP samples from Hdh striatal cells with 10μM PD98059 (MEK1/2 inhibitor) and 1μM δV1-1 (PKCδ inhibitor) treatment. Phosphorylation level was quantified compared to total Drp1 level, n=2 **(D-F)** Serine/threonine phosphorylation of Drp1 from input samples from HeLa epithelial cells with 10μM PD98059 and 1μM δV1-1 treatment. Phosphorylation level was quantified compared to total Drp1 level, n=2

There were three issues with this kinase inhibitor experiment that led to an adjustment in protocol. First, PD98059 did not give consistent results, so U0126, a more potent and selective MEK1/2 inhibitor, was used going forward. Second, immunoprecipitation of Drp1, after kinase inhibitor treatment, did not show the difference in overall serine/threonine phosphorylation between wild-type and mutant cells, so just input samples were analyzed going further. Third, after the identification of the serine site of Drp1 that is phosphorylated in models of HD, only that serine site's phosphorylation was analyzed with the new MEK1/2 inhibitor. Since there are multiple serine and threonine sites on Drp1 it was difficult to distinguish changes in overall serine/threonine phosphorylation when just one serine site was being modified.

2.2 In vitro phosphorylation results

MAPK1 binds to and phosphorylates Drp1 in vitro

Our lab has shown that MAPK1 is the leading kinase to interact with Drp1 in striatal cells derived from HD patient-iPS cells through mass spectrometry analysis of Drp1's interactome. In order to determine whether or not Drp1 is a substrate for MAPK1 phosphorylation, an *in vitro* phosphorylation assay was performed and analyzed using the western blot technique. 500ng of human recombinant Drp1 was incubated with 250ng of human recombinant MAPK1 in 30μL of reaction mixture

(containing ATP). The immunoprecipitation of Drp1 shown in **Figure 7A** confirms that Drp1 and MAPK1 interact (**lane 2**); however, the presence of MAPK1 in **lane 4**, when there was no Drp1 present in the sample to be immunoprecipitated, led to the validation of Drp1 and MAPK1 interaction by immunopecipitating MAPK1 (**Figure 7B**). Western blot analysis shows phosphorylation of Drp1 only in the presence of MAPK1 (**Figure 7C, lane 2**). The *in vitro* phosphorylation assay further supports our observation above that MAPK1 directly binds to and phosphorylates Drp1.

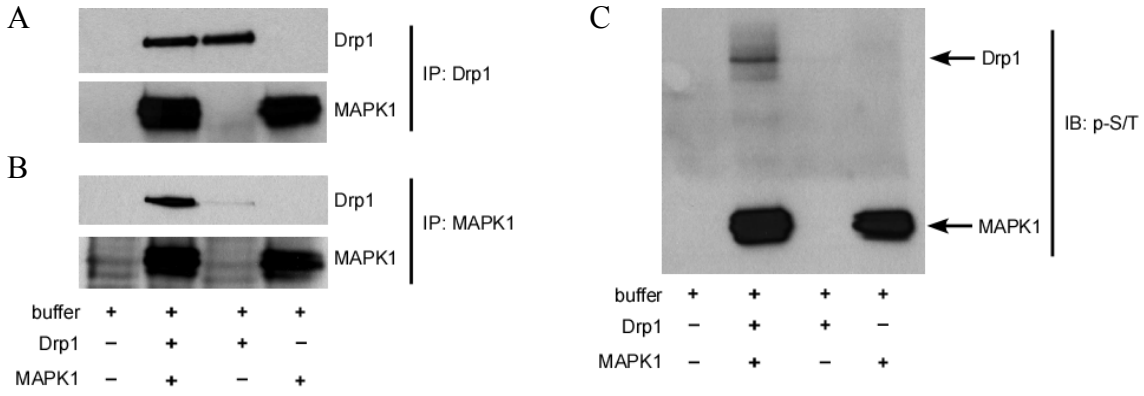

Figure 7. *In vitro* phosphorylation assay of Drp1 and MAPK1. **(A-B)** Western blot analysis of immunoprecipitation of Drp1 (n=1) and MAPK1 (n=1) using antibodies to Drp1 and MAPK1. **(C)** Western blot analysis using an antibody to p-S/T, n=2.

In vitro phosphorylation assay for mass spectrometry analysis identified six serine residues on Drp1 phosphorylated by MAPK1

Next, to determine what serine/threonine sites on Drp1 are phosphorylated by MAPK1 another *in vitro* phosphorylation assay was performed, this time with 1µg of human recombinant Drp1 and 500ng of human recombinant MAPK1 (in duplicates) in 30µL of reaction mixture (containing ATP). The samples were then

separated by SDS-PAGE, and the gel was stained with Coomassie blue. **Figure 8** is a picture of the gel that was sent to the Mass Spectrometry Laboratory for Protein Sequence at Cleveland Clinic Foundation (CCF).

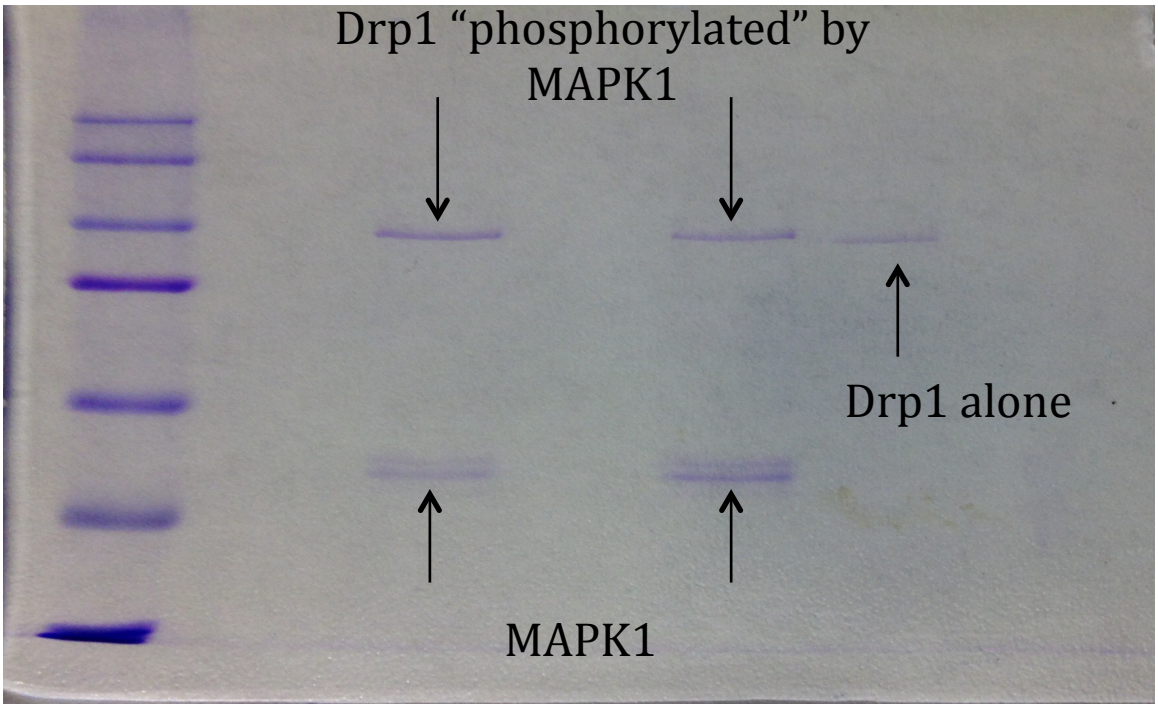

Figure 8. SDS-PAGE gel with Coomassie blue staining for mass spectrometry analysis.

At CCF the two "phosphorylated Drp1" bands were excised from the gel, reduced and then alkylated. One band was digested with trypsin and the other band was digested with chymotrypsin. HPLC (high performance liquid chromatography) using a reverse phase capillary chromatography column was used to separate the peptides produced from the trypsin (55 peptides, **Supplemental Figure A1**) and chymotrypsin (159 peptides, **Supplemental Figure A2**) digests. A total of 14 phosphopeptides were identified and tandem mass spectrometry (MS/MS) was used to identify six phosphorylation sites (**Supplemental Figures A3-A8**). The

relative abundance of the six phosphorylation sites was estimated by using the chromatograms of the modified and unmodified form of each phosphopeptide to calculate peak area ratio (PA (phospho)/PA (unmodified); **Figure 9**).

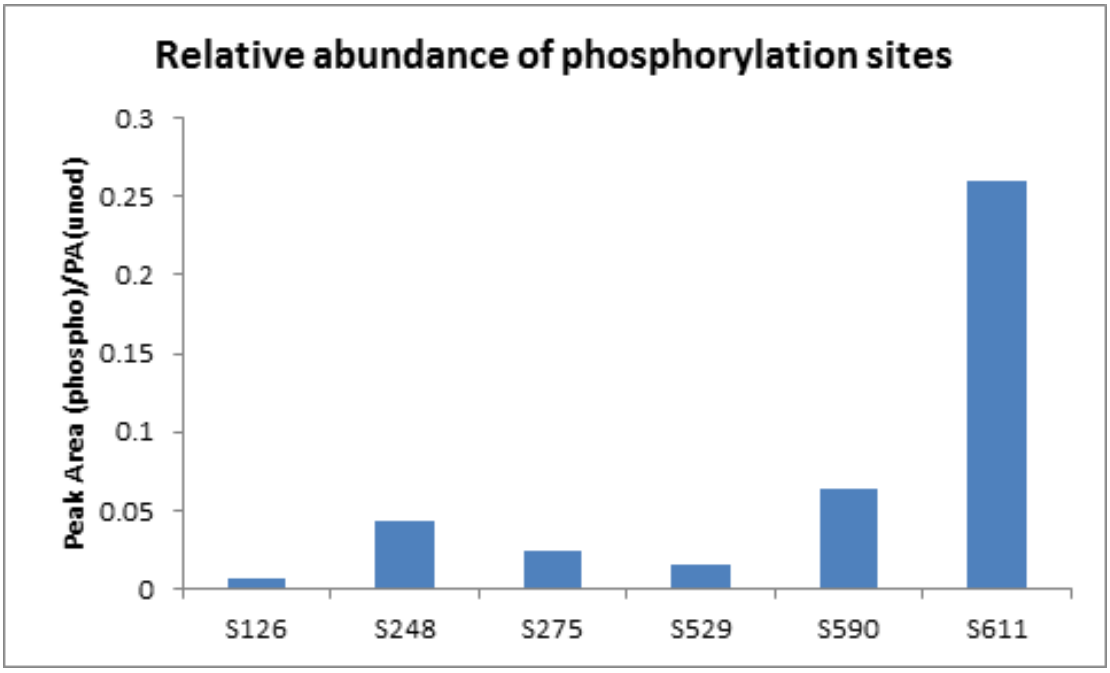

Figure 9. Relative abundance of Drp1 phosphorylation sites targeted by MAPK1. Drp1 isoform 2.

With six possible phosphorylation sites of Drp1 targeted by MAPK1 *in vitro* three criteria were used to prioritize which serine sites to investigate as the possible phosphorylation site of Drp1 in HD. First, the relative abundance of the six phosphorylation sites was taken into consideration, with the top three being S637, S616, and S248 (isoform 1, **Figure 9**, **Table 1**). Second, the domain of Drp1 (**Table 1**) should be taken into consideration. S248 is in the middle domain (**Figure 3**, green), S616 is in the variable domain (**Figure 3**, green), and S637 is in the GTPase effector domain (GED, **Figure 3**, red). Of note, phosphorylation in the GED inhibits

intramolecular interactions between the GED domain and the GTP binding/middle domain that is important for GTPase activity, and is thus considered to have a protective role on mitochondria. Third, literature shows S616 and S637 as the two main serine residues that when phosphorylated by different kinases has an effect on the activity of the GTPase.[51, 53-55] Since phosphorylation at S616 and S637 has opposite effects on Drp1's GTPase activity, these two serine sites will be investigated first to determine which one, if either, has an elevated phosphorylation in HD, compared to wild-type.

Isoform 1	Isoform 2	Isoform 3	Domain
S126	S126	S126	GTPase binding domain
S248	S248	S248	Middle domain
S275	S275	S275	Middle domain
S529	S529	S529	Variable domain
S616	S590	S579	Variable domain
S637	S611	S600	GED domain

Table 1. Serine residues phosphorylated by MAPK1 and their domain. Drp1 isoform 1-3 serine site comparison.

2.3 Identifying the site of Drp1 phosphorylation in HD and the role MAPK1 inhibition has on cell signaling in HD

Drp1 has an increased Ser616 phosphorylation in mutant HdhQ111 striatal cells compared to wild-type HdhQ7 striatal cells, with no change in Ser637 phosphorylation

In order to determine the phosphorylation level of Drp1 at specific serine sites total lysates were harvested from the Hdh mouse striatal cells and western blot analysis was performed. The membrane was probed with anti-p-Drp1 S616, anti-p-Drp1 S637, and anti-Drp1. Analysis revealed that Drp1 has an increased Ser616

phosphorylation (**Figure 10A, B**) in mutant HdhQ111 striatal cells compared to wild-type HdhQ7 striatal cells, with no change in Ser637 phosphorylation (**Figure 10C, D**) between mutant HdhQ111 striatal cells and wild-type HdhQ7 striatal cells. This new result identifies a serine site of Drp1 phosphorylated in this HD model that can explain the excessive mitochondrial fragmentation that is observed in HD models, since Ser616 is known to increase the protein's GTPase activity.

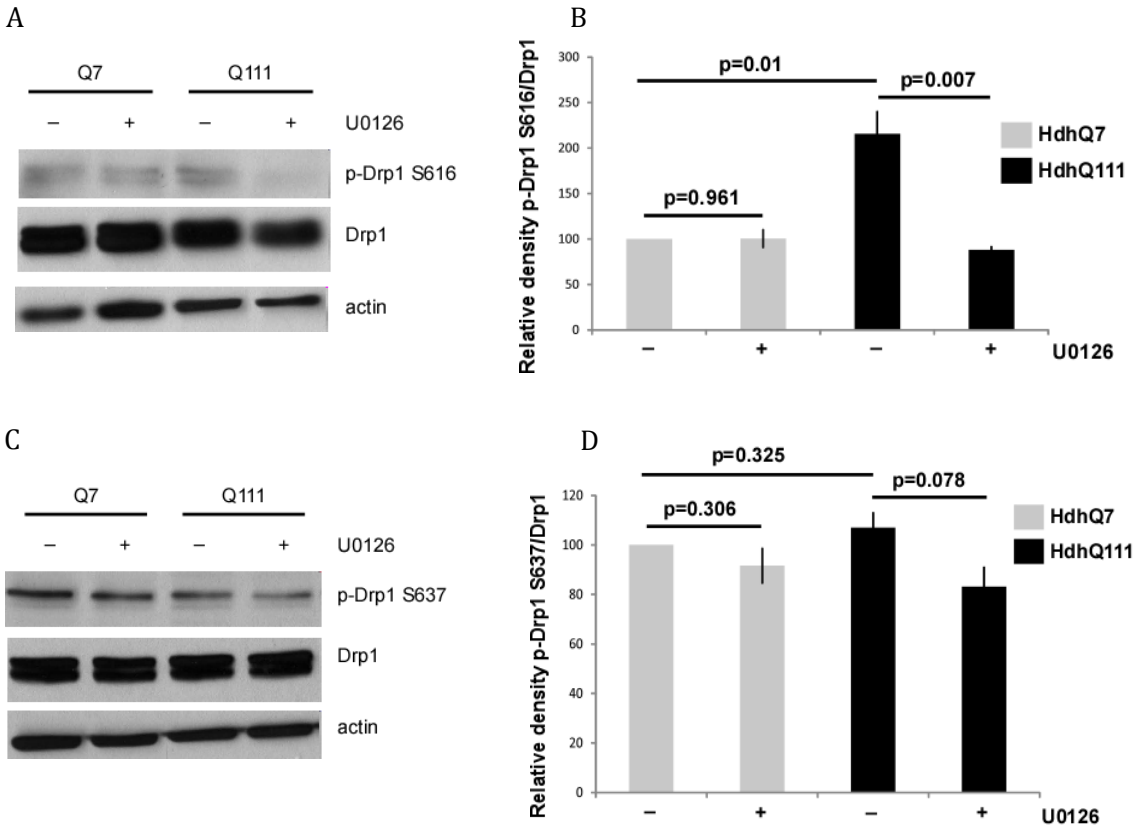

Figure 10. Ser616 and Ser637 phosphorylation of Drp1 in HD and the effect of MAPK1 inhibition. **(A-B)** Ser616 phosphorylation in Hdh striatal cells with and without 10μM U0126 treatment. Phosphorylation level was quantified compared to total Drp1 level, n=3 **(C-D)** Ser637 phosphorylation in Hdh striatal cells with and without 10μM U0126 treatment. Phosphorylation level was quantified compared to total Drp1 level, n=3

MAPK1 inhibition decreased Ser616 phosphorylation of Drp1 in mutant HdhQ111 striatal cells, with no significant change in Ser637 phosphorylation

Next, to determine what, if any, role MAPK1 plays in the phosphorylation of Drp1, Hdh striatal cells were treated with DMSO (control) or 10μM U0126 (MEK1/2 inhibitor) for four hours. After treatment total lysates were harvested from the Hdh mouse striatal cells and analyzed with the western blot technique. The membrane was probed with anti-p-Drp1 S616, anti-p-Drp1 S637, and anti-Drp1. Analysis revealed that the increased Ser616 phosphorylation of Drp1 that is observed in mutant HdhQ111 striatal cells was decreased with inhibition of MAPK1 (**Figure 10A, B**), with no effect on Ser616 phosphorylation in wild-type HdhQ7 striatal cells. Western blot analysis also revealed that inhibition of MAPK1 had no significant change in Ser637 phosphorylation for either mutant HdhQ111 striatal cells or wild-type HdhQ7 striatal cells (**Figure 10C, D**). The effect inhibition of MAPK1 has on Drp1 phosphorylation at Ser616 suggests that MAPK1 plays a role in the activation of Drp1 in HD.

Drp1 tetramer is increased in mutant HdhQ111 striatal cells, but MAPK1 has no effect on the oligomerization of Drp1

To further investigate the mechanism underlying Drp1 activation by MAPK1 in HD the oligomerization of Drp1 was investigated and the role that MAPK1 plays

in the formation of the Drp1 tetramer. Formation of Drp1 tetramer at constriction sites on the outer mitochondrial membrane has been shown to be required for mitochondrial fission, by accelerating the GTP hydrolysis necessary to sever the mitochondrial membrane.[31] Hdh striatal cells were treated with DMSO or 10μM U0126 for four hours before total lysates were harvested. Samples were resuspended in sample loading buffer without β-mercaptoethanol to maintain cysteine-cysteine linkages between Drp1 molecules. The membrane was probed with anti-Drp1 and western blot analysis shows an increase in the formation of the Drp1 tetramer (**Figure 11A, B**) in mutant HdhQ111 striatal cells compared to wild-type HdhQ7 striatal cells. However, also shown in **Figure 11A, B** one can see that inhibition of MAPK1 has no effect on formation of the Drp1 tetramer in either mutant HdhQ111 or wild-type HdhQ7 striatal cells. These results indicate that although Drp1 tetramer formation is increased in HD, MAPK1 plays no role in its formation.

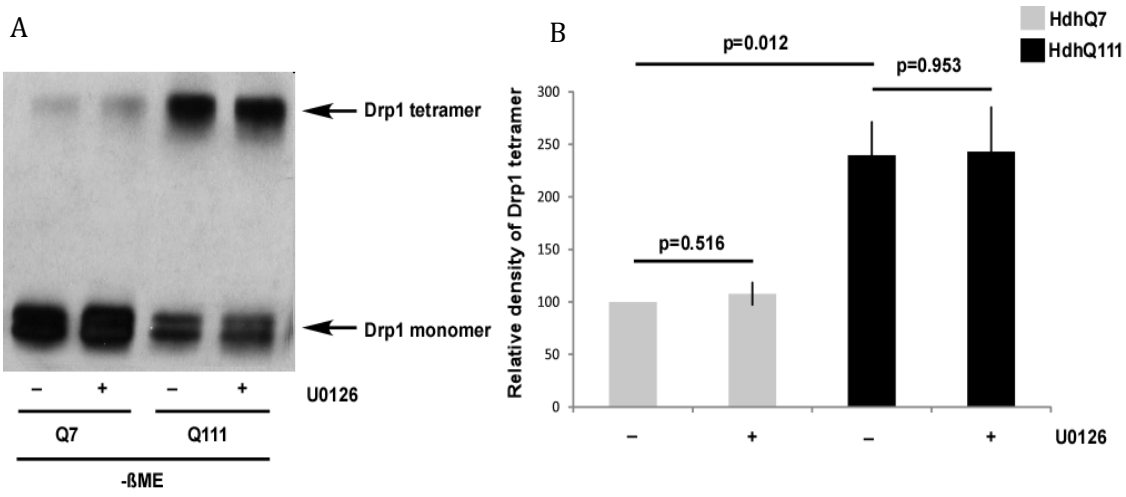

Figure 11. Drp1 oligomerization in HD and the effect of MAPK1 inhibition. **(A)** Hdh striatal cells were treated with 10μM U0126 and after total lysates were harvested samples were resuspended in sample loading buffer without β-mercaptoethanol to maintain cysteine-cysteine bond linkage between Drp1 molecules. **(B)** Drp1 tetramer quantification, n=3

2.4 The effect of MAPK1 inhibition on mitochondrial morphology, mitochondrial function, and neuronal cell death in HD

MAPK1 inhibition significantly decreased the amount of mitochondrial fragmentation that is observed in mutant HdhQ111 striatal cells

To better understand the functional significance of Drp1 phosphorylation at Ser616 by MAPK1, mitochondrial fragmentation was examined *in vitro*. Hdh striatal cells were plated on coated coverslips and then treated with DMSO or 10μM U0126 for 16 hours. Striatal cells were incubated with anti-Tom20, specific to a protein on the outer mitochondrial membrane, and then the secondary antibody FITC-labeled goat anti-rabbit for the green fluorescence shown in **Figure 12A**. Confocal analysis shows wild-type HdhQ7 striatal cells with elongated mitochondria, forming a

diverse network throughout the striatal cell. Mutant HdhQ111 striatal cells show atypical mitochondrial fragmentation in the processes with perinuclear localization of the mitochondria in the cell body. However, after treatment with U0126 mutant HdhQ111 striatal cells show more elongated mitochondria with a more diverse mitochondrial network in the processes of the striatal cells with less perinuclear localization. The results are summarized in the histogram in **Figure 12B**, showing a greater percent of mutant HdhQ111 striatal cells fragmented, compared to wild-type HdhQ7 striatal cells, as well as the decrease in fragmentation that is observed in mutant HdhQ111 striatal cells with U0126 treatment. This result suggests that MAPK1 plays a role in the mitochondrial fragmentation that is observed in this cell culture model of HD.

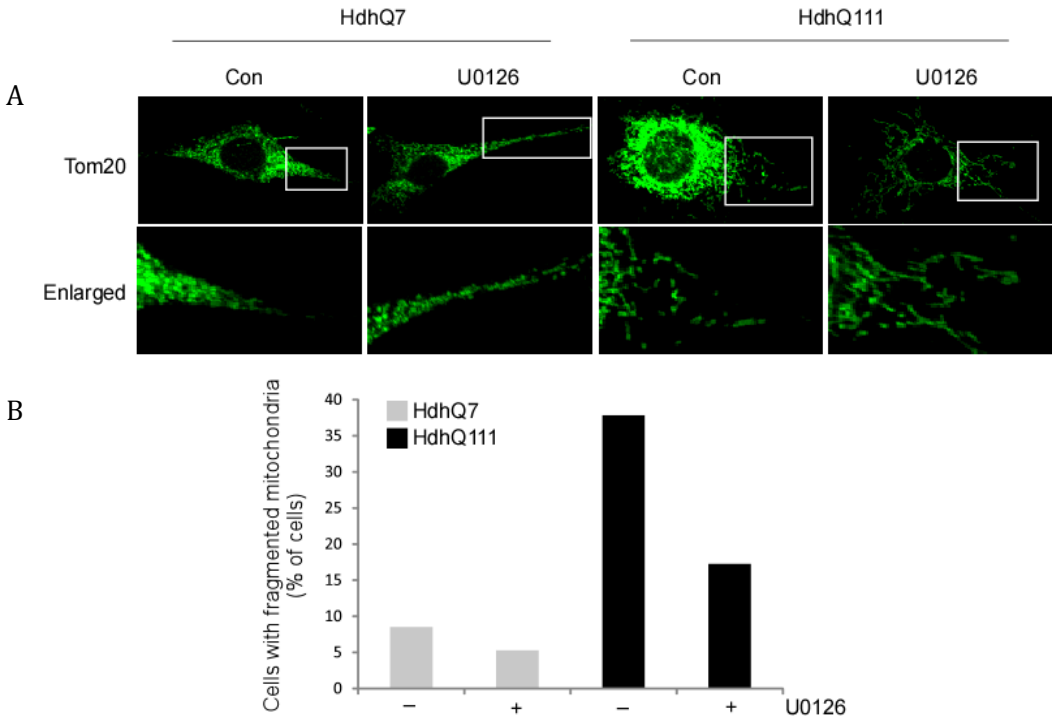

Figure 12. The effect MAPK1 inhibition has on mitochondrial fragmentation in HD. **(A)** Hdh striatal cells treated with DMSO or 10μM U0126 for 16 hours. Striatal cells were stained for the outer mitochondrial membrane protein, Tom20, to evaluate mitochondrial morphology. **(B)** Histogram of % of total cells with fragmented mitochondria. At least 100 cells for each group were analyzed from two separate experiments.

MAPK1 inhibition restored the mitochondrial membrane potential, as well as decreased the superoxide production in mutant HdhQ111 striatal cells

Mitochondrial fragmentation leads to the permeabilization of the outer mitochondrial membrane, decreasing the mitochondrial membrane potential and causing the release of ROS.[51] Therefore, to determine the effect inhibition of MAPK1 has on mitochondrial function, mitochondrial membrane potential and mitochondrial superoxide production was examined *in vitro*. Hdh striatal cells were plated on coated coverslips and then treated with DMSO or 10μM U0126 for 16

hours. To determine the effect inhibition of MAPK1 has on mitochondrial membrane potential, striatal cells were incubated with 0.25μM tetramethylrhodamine (TMRM, **Figure 13**) for 20 minutes at 33°C. To determine the effect inhibition of MAPK1 has on mitochondrial ROS (mitoRos) production, striatal cells were incubated with 5μM of the mitochondrial superoxide indicator MitoSox™ (**Figure 14**) for 10 minutes at 33°C. Confocal analysis shows mutant HdhQ111 striatal cells with a decreased mitochondrial membrane potential, compared to wild-type HdhQ7 striatal cells, with restoration of the membrane potential in mutant HdhQ111 striatal cells after U0126 treatment (**Figure 13A, B**). Confocal analysis also shows mutant HdhQ111 striatal cells with an increased superoxide production, compared to wild-type HdhQ7 striatal cells, with a decrease in MitoROS in mutant HdhQ111 striatal cells after U0126 treatment (**Figure 14A, B**). Of note, U0126 treatment increased MitoROS production in wild-type HdhQ7 striatal cells. This may be due to the fact that in a normal physiological state inhibiting MAPK1 has a deleterious effect on mitochondrial function. The restoration of mitochondrial membrane potential, and decrease in MitoROS in mutant HdhQ111 striatal cells with U0126 treatment suggests that MAPK1 plays a role in the mitochondrial dysfunction that is observed in this cell culture model of HD.

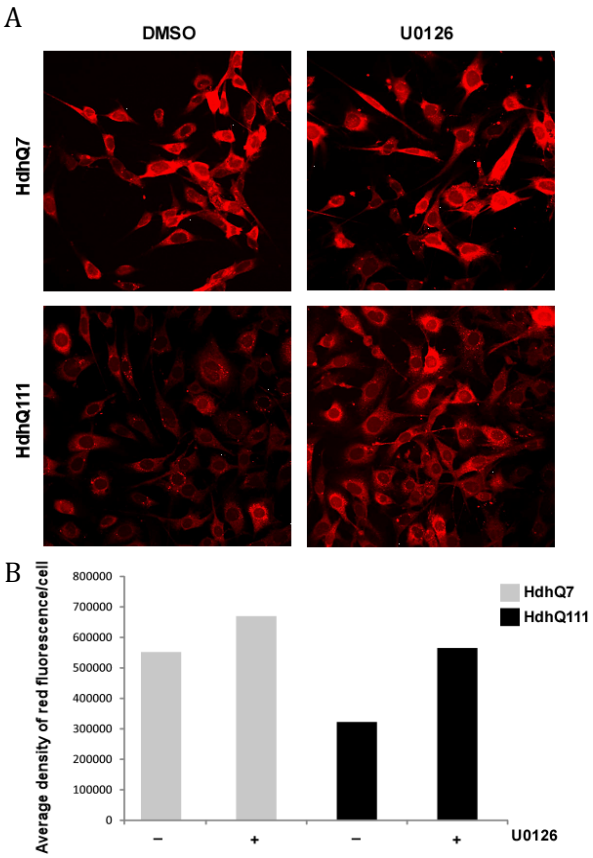

Figure 13. The effect MAPK1 inhibition has on mitochondrial membrane potential in HD. **(A)** Hdh striatal cells treated with DMSO or 10μM U0126 for 16 hours. Striatal cells were stained with tetramethylrhodamine (TMRM) to determine the mitochondrial membrane potential. **(B)** Histogram of average density of red fluorescence/cell. At least 100 cells for each group were analyzed from two separate experiments.

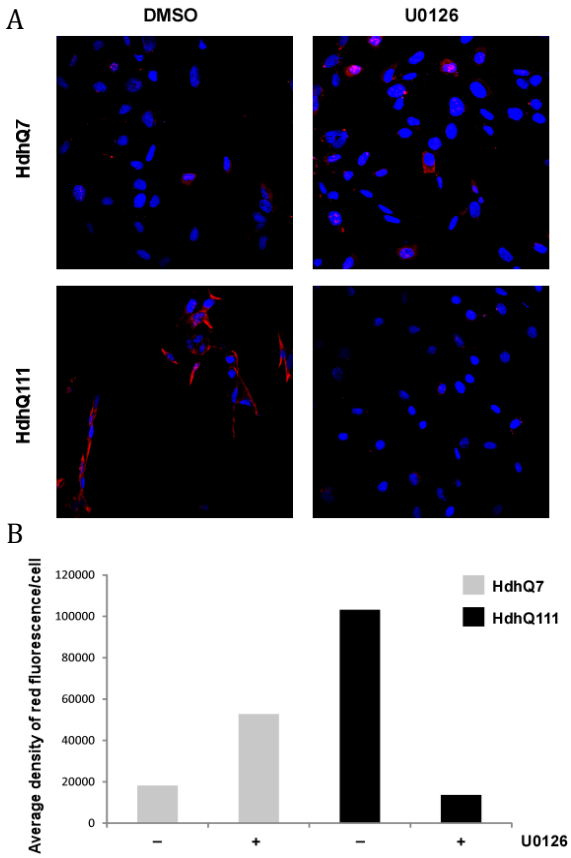

Figure 14. The effect MAPK1 inhibition has on mitochondrial ROS production in HD. **(A)** Hdh striatal cells treated with DMSO or 10μM U0126 for 16 hours. Striatal cells were stained with mitochondrial superoxide indicator MitoSox to determine the mitochondrial superoxide production. **(B)** Histogram of average density of red fluorescence/cell. Approximately 100 cells for each group were analyzed from two separate experiments.

MAPK1 inhibition slowed down neuronal cell death in mutant HdhQ111 striatal cells, but did not significantly decrease cell death

To better understand the consequences mitochondrial fragmentation and mitochondrial dysfunction has in HD, neuronal cell death was investigated. Hdh mouse striatal cells were serum depleted for 8 hours, followed by treatment with DMSO or 10/25/50μM U0126 for 16 hours in fresh DMEM medium minus serum (for a total of 24 hours of serum starvation). Medium and total cell lysates were collected at the end of treatment. A cytotoxicity kit from Roche was used to determine the amount of lactate dehydrogenase (LDH, an indicator for cell death)

that was released from the striatal cells. **Figure 15** shows that serum starvation induces cell death in both wild-type HdhQ7 and mutant HdhQ111 striatal cells, but more so in mutant HdhQ111 striatal cells. U0126 slowed down striatal cell death in mutant HdhQ111 cells in a dose dependent manner with 10μM U0126 (**Figure 15A**) having no significant decrease, 25μM U0126 (**Figure 15B**) decreasing cell death by 8%, and 50μM U0126 (**Figure 15C**) decreasing cell death by 14%. Of note, cell death increased in wild-type HdhQ7 striatal cells with both 10μM U0126 (**Figure 15A**) and 25μM U0126 (**Figure 15B**) treatment. There are a few possible explanations for why inhibition of MAPK1 does not significantly decrease striatal cell death in this model of HD. First, the 16-hour treatment might not be long enough for the reversed mitochondrial dysfunction to have any effect on neuronal survival. Second, since serum starvation occurred before U0126 treatment, perhaps all the inhibitor could do was slow down cell death. One might adjust the protocol to see if treatment with U0126 prior to serum starvation protected the cells, therefore, more significantly decreasing cell death in mutant HdhQ111 striatal cells. Third, since MAPK1 is a part of an intricate cell-signaling pathway, with multiple cellular targets and effects, inhibition of MAPK1 may have other deleterious effects on neuronal survival.

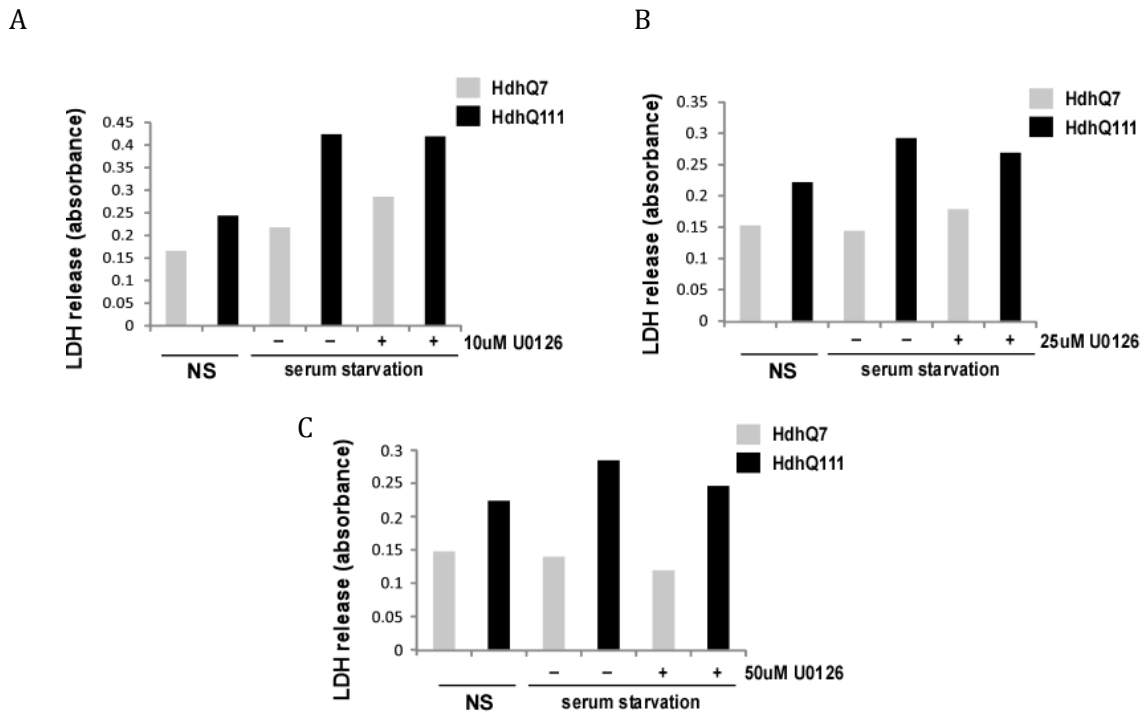

Figure 15. The effect MAPK1 inhibition has on neuronal cell death in HD. Hdh striatal cells were serum depleted for 24 hours to induce cell death. Histograms show the amount of lactate dehydrogenase (LDH) released from striatal cells, which is an indicator for cell death. **(A)** Hdh striatal cells were treated with 10μM U0126 for 16 hours, n=2 **(B)** Hdh striatal cells were treated with 25μM U0126 for 16 hours, n=2 **(C)** Hdh striatal cells were treated with 50μM U0126 for 16 hours, n=2

The phosphorylation-deficient mutant of Drp1, Ser616Ala, decreased mitochondrial fragmentation in mutant HdhQ111 striatal cells

In order to determine if phosphorylation of Drp1 at Ser616 plays a role in the mitochondrial fragmentation observed in models of HD a phosphorylation-deficient mutant, Ser616Ala, of Drp1 was created. Mutant HdhQ111 striatal cells were transfected with the phosphorylation-deficient mutant tagged to myc, using the transfection agent *Trans*IT 2020 for 42 hours. Striatal cells were incubated with anti-Tom20 and anti-myc, to identify the mitochondrial morphology and the striatal

cells transfected with Drp1 S616A mutant, respectively. Then the secondary antibody rhodamine-labeled goat anti-rabbit for the red fluorescence was used for Tom20 and the secondary antibody FITC-labeled goat anti-mouse for the green fluorescence was used for myc-Drp1-S616A as shown in **Figure 16A**. Confocal analysis shows mutant HdhQ111 striatal cells, which have been transfected with myc-Drp1-S616A mutant, with elongated mitochondria, a more diverse mitochondrial network, and less perinuclear mitochondrial localization. This suggests that phosphorylation of Drp1 at Ser616 plays a role in mitochondrial fragmentation that is observed in models of HD. The results summarized in the histogram in **Figure 16B** show that although the Drp1-S616A phosphorylation-deficient mutant decreased fragmentation in mutant HdhQ111 striatal cells, it did not decrease fragmentation as much as U0126 treatment did. This can be explained by the low efficiency of transfection of the phosphorylation-deficient mutant, as well as the presence of endogenous Drp1 that can still be phosphorylated by MAPK1. Two possible adjustments can be made for future experiments. First, before transfection, use short interfering RNA (siRNA) to silence endogenous Drp1. However, the efficiency of siRNA is just as low as transfection, and you cannot guarantee that a striatal cell will get both siRNA and the transfected mutant. Second, you can use a Drp1 knockout (KO) model to ensure that the only Drp1 present is the transfected mutant. However, Drp1 KO cells are not considered to be a model for HD.

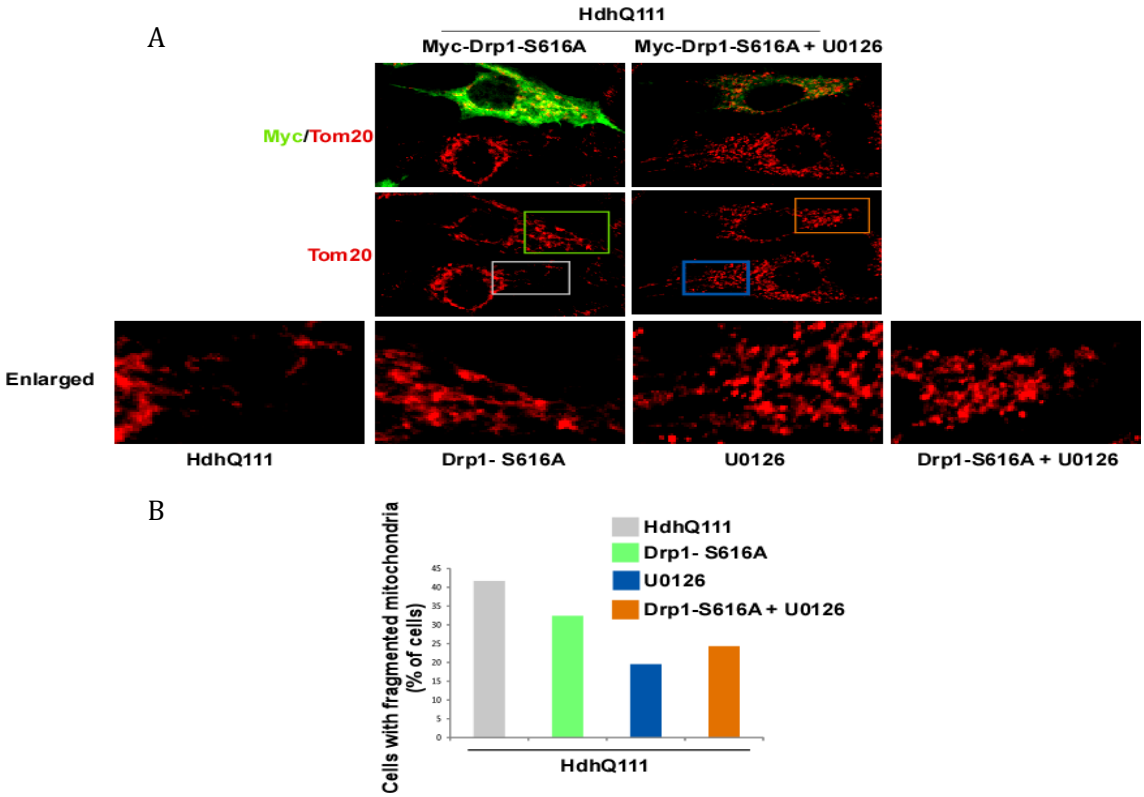

Figure 16. The role Drp1 Ser616 plays in mitochondrial fragmentation in HD. **(A)** Hdh striatal cells transfected with S616A mutant ± 10μM U0126 for 16 hours. Striatal cells were stained with Tom20 (red) to evaluate mitochondrial morphology and with myc (green) to determine which cells were transfected with the Drp1 S616A mutant. **(B)** Histogram of % of total cells with fragmented mitochondria. At least 100 cells for each group were analyzed from one individual experiment.

Mutant HdhQ111 striatal cells transfected with Drp1 S616A mutant and treated with a MEK1/2 inhibitor decreased mitochondrial fragmentation to the same degree as treatment with a MEK1/2 inhibitor alone

Lastly, to determine if phosphorylation of Drp1 at Ser616 and MAPK1 act through the same pathway the combined effect that a Drp1 phosphorylation-deficient mutant plus inhibition of MAPK1 has on mitochondrial fragmentation was investigated *in vitro*. Mutant HdhQ111 striatal cells were transfected with the

phosphorylation-deficient mutant tagged to myc, using the transfection agent *Trans*IT 2020 for 26 hours. Striatal cells were then treated with 10μM U0126 for 16 hours. Striatal cells were incubated with anti-Tom20 and anti-myc. Then the secondary antibody rhodamine-labeled goat anti-rabbit for the red fluorescence was used for Tom20 and the secondary antibody FITC-labeled goat anti-mouse for the green fluorescence was used for myc-Drp1-S616A, as shown in **Figure 16A**. Confocal analysis shows that mutant HdhQ111 striatal cells that have been transfected with myc-Drp1-S616A mutant and exposed to U0126 treatment had the same degree of mitochondrial elongation as mutant HdhQ111 striatal cells that had just been exposed to U0126 treatment. This finding, summarized in the histogram in **Figure 16B**, suggests that MAPK1 and Ser616 phosphorylation of Drp1 are a part of the same pathway that leads to the mitochondrial fragmentation and mitochondrial dysfunction observed in this model of HD.

In summary (Figure 17), MAPK1 phosphorylates Drp1 at Ser616 increasing mitochondrial fission in HD, but not through the formation of Drp1 tetramer that is essential for GTP hydrolysis. More experiments should be done to further understand the mechanism underlying how phosphorylation of Drp1 at Ser616 by MAPK1 leads to increased mitochondrial fission. The role MAPK1 plays in Drp1 translocation to the mitochondria and activity of the GTPase has yet to be explored. The phosphorylation of Drp1 at Ser616 by MAPK1 leads to the mitochondrial fragmentation, decreased mitochondrial membrane potential, and increased superoxide production observed in HD. However, the role MAPK1 plays in neuronal

cell death in HD is still unclear and requires further investigation.

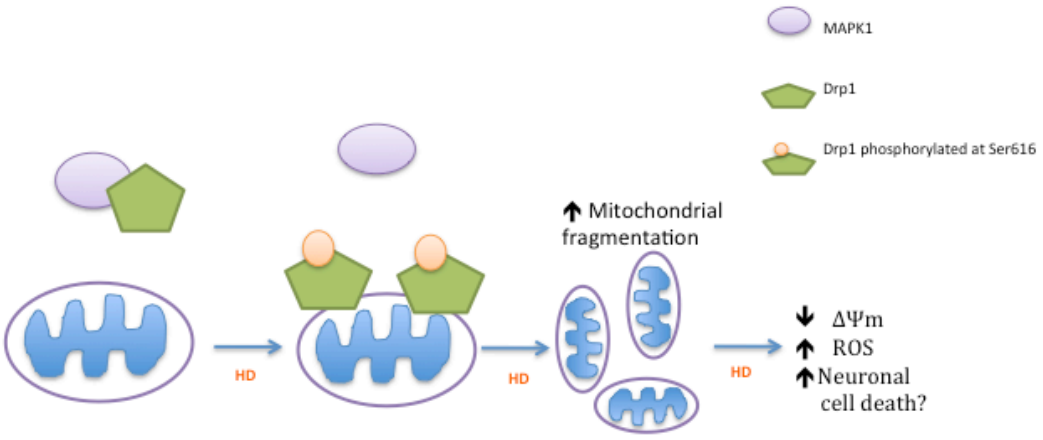

Figure 17. Summary of Drp1 activation by MAPK1 leading to the mitochondrial fragmentation observed in HD. ERK2 (MAPK1) phosphorylates Drp1 at Ser616 causing hyper-fission and increased mitochondrial fragmentation that leads to a decrease in the mitochondrial membrane potential and increased MitoROS production. The mechanism behind the increased fission activity of Drp1 by MAPK1 still requires further investigation and the effect MAPK1 has on neuronal cell death in HD also requires further investigation.

CHAPTER III: MATERIALS AND METHODS

3.1 In vitro phosphorylation assay

Recombinant human MAPK1 (250ng, Prospec) and recombinant human Drp1 (500ng, Abnova) were incubated in 30µL of reaction mixture (40mM Tris-HCl pH 7.5, 2mM dithiothreitol (DTT), 10mM $MgCl_2$, 100µM ATP) at 30°C for 30 minutes. To one set of samples, sample loading buffer was added, followed by boiling at 100°C for five minutes, and then stored at -20°C. To the second set of samples, 500µL of reaction mixture/sample (+) 3µL of antibody/sample for immunoprecipitation (either anti-Drp1 or anti-MAPK1) was added and then incubated at 4°C overnight. 30µL of protein A/G beads were then added to the immunoprecipitates and incubated for one hour. The immunoprecipitates were washed 4X using reaction mixture minus ATP, then 15µL of sample loading buffer was added, and samples were boiled at 100°C. Both sets of samples were then subjected to 10% SDS-PAGE followed by immunoblotting with Drp1 antibodies (BD Transduction) and ERK1/2 antibodies (MAPK1, Proteintech) for the IP samples and phospho-(Ser/Thr) antibodies (Cell Signaling) for the input samples.

3.1.1 Mass spectrometry analysis

Two sets of recombinant human MAPK1 (500ng, Prospec) and recombinant human Drp1 (1µg, Abnova) were incubated in 30µL of reaction mixture (40mM Tris-

HCl pH 7.5, 2mM DTT, 10mM $MgCl_2$, 100μM ATP) at 30°C for 30 minutes. To stop the reaction sample loading buffer was added, followed by boiling at 100°C for five minutes. Both sets of samples were then subjected to 10% SDS-PAGE followed by Coomassie blue staining. The gel was then sent to the Mass Spectrometry Laboratory for Protein Sequence at Cleveland Clinic Foundation (CCF). At CCF, the bands were excised from the gel, washed/destained in 50% ethanol with 5% acetic acid, dehydrated in acetonitrile, reduced with DTT, alkylated with iodoacetamide, and digested with either trypsin or chymotrypsin. After complete digestion the peptides were extracted from the polyacrylamide using 50% acetonitrile with 5% formic acid. The digest was analyzed by capillary column liquid chromatography-tandem mass spectrometry (LC-MS).

3.2 Cell model and cell culture

Hdh mouse striatal cells have been previously described[62] and were derived from a knock-in transgenic mouse model with either 7-polyglutamine repeats (Q7, wild-type) or 111-polyglutamine repeats (Q111, HD) in the *Huntingtin gene*. These cells were maintained in HyClone™ Dulbecco's modified Eagle's medium (DMEM, GE Healthcare Life Sciences) supplemented with 10% fetal bovine serum (FBS, Corning), 1% penicillin/streptomycin, and 0.4mg/mL G418. Cultures were maintained at 33°C in a humidified atmosphere containing 5% CO_2.

HeLa human epithelial cells were derived from cervical carcinoma cells and have been previously described.[63] The HeLa cells have been transfected with myc-

tagged plasmids containing either 23-polyglutamine repeats (Q23, wild-type) or 73-polyglutamine repeats (Q73, HD). These cells were maintained in HyClone™ DMEM (GE Healthcare Life Sciences) supplemented with 10% FBS (Corning), 1% penicillin/streptomycin, and 0.4mg/mL G418. Cultures were maintained at 35°C in a humidified atmosphere containing 5% CO_2.

3.3 Kinase inhibitor treatment

To determine the effect of MAPK1 on Drp1 phosphorylation in HD, striatal cells were treated with 10μM U0126 (InvivoGen) for four hours in fresh DMEM medium before total lysates were obtained for western blot analysis. To determine the effect MAPK1 has on mitochondrial morphology and function in HD, striatal cells were plated on coverslips coated in a gelatin/fibronectin mixture, treated with 10μM U0126 for 16 hours in fresh DMEM medium, and then cells were stained and imaged using a confocal microscope (Olympus, Fluoview FV100). To determine the effect MAPK1 has on cell death in HD, striatal cells were treated with 10/25/50μM U0126 for 16 hours. As shown in **Figure 18,** U0126 is an inhibitor of MAP kinase kinases MEK1 and MEK2. This prevents the activation of ERK2 (MAPK1/MAP kinase p42), thus preventing the phosphorylation of Drp1 in HD.

Other kinase inhibitors used: PD98059 (Tocris) is a MEK1/2 inhibitor that's means of action is the same as U0126 depicted in **Figure 18**. PD98059 was used at 10μM for one hour. δV1-1 (American Peptide) is a selective PKCδ peptide inhibitor

that inhibits PKCδ translocation to the cell membrane, thus preventing its activation. δV1-1 was used at 1μM for one hour.

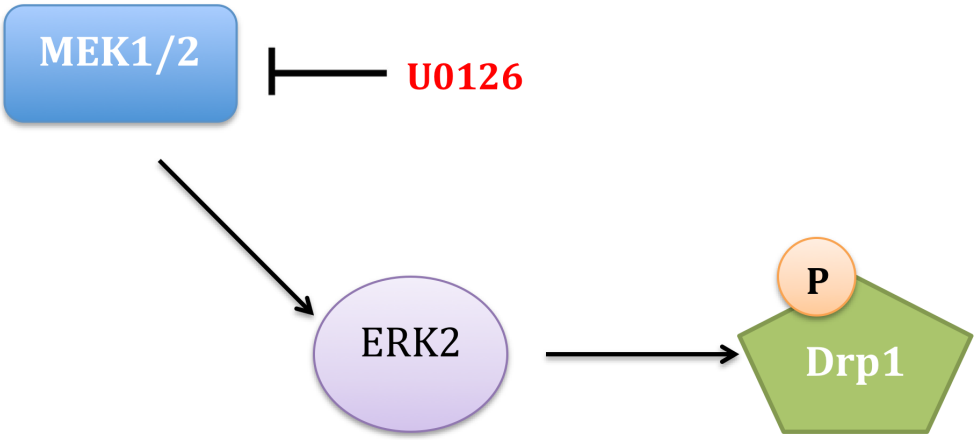

Figure 18. Schematic of U0126 inhibition of Drp1 phosphorylation by ERK2 (MAPK1).

3.4 Harvesting total lysates and immunoprecipitation of Drp1

Hdh mouse striatal cells were washed with 1X PBS and then incubated in total lysis buffer (10mM HEPES-NaOH pH 7.8, containing 150mM NaCl, 1mM EGTA, 1% Triton X-100, protease inhibitor, and phosphatase inhibitor) for 20 minutes at 4°C. Cells were scraped and then homogenized 5X using a 25-gauge syringe. Samples were centrifuged at 12,000g for 20 minutes at 4°C. Supernatants were saved as total lysates (stored at -20°C) and the pellet was discarded. After protein concentrations were determined using the Bradford assay described previously[56] 800μg of soluble protein was incubated with 3μL of anti-Drp1 (BD Transduction) overnight at 4°C followed by 30μL of protein A/G beads (Santa Cruz) for one hour.

Immunoprecipitates were washed 4X using total lysis buffer minus inhibitors, separated by 10% SDS-PAGE, and then probed with phospho-(Ser/Thr) antibodies (Cell Signaling) and ERK1/2 polyclonal antibodies (Proteintech).

3.5 Western blot analysis

Total lysates were prepared as described above. Protein concentrations were determined using the Bradford assay. Then 30-40μg samples were resuspended in sample loading buffer, boiled at 100°C for five minutes, and separated by 10% SDS-PAGE. Protein was transferred onto a nitrocellulose membrane, probed using the antibodies shown in **Table 2**, and visualized using ECL solution. Band densities were analyzed using NIH ImageJ software. Histograms show the relative density of the protein of interest/the total amount of Drp1*. Densities of the wild-type, control, cells were standardized to 100% (density of wild-type/density of wild-type x 100) and the densities for other samples were then determined as the percent of wild-type, control (density of mutant/density of wild-type x 100).

To determine the effect U0126 inhibitor has on Drp1 oligomerization samples were resuspended in sample loading buffer without β-mercaptoethanol and then separated by 8% SDS-PAGE.

*Exception- Figure 11, Drp1 tetramer- just relative density of Drp1 tetramer

Primary Antibody	Company	Dilution (Western)	Dilution (Immunostaining)	Secondary Antibody
Phospho-(Ser/Thr)*	Cell Signaling	1:1000	--	Rabbit
Phospho-Drp1 S616*	Cell Signaling	1:1000	--	Rabbit
Phospho-Drp1 S637*	Cell Signaling	1:1000	--	Rabbit
DLP1 (Drp1)	BD Transduction	1:1000	--	Mouse
ERK1/2 (MAPK1)	Proteintech	1:1000	--	Rabbit
β-actin	Santa Cruz	1:10,000	--	Mouse
Myc	Santa Cruz	1:2000	1:500	Mouse
Tom20	Santa Cruz	--	1:500	Rabbit

Table 2. List of antibodies
*Phosphorylated antibodies were prepared in 3% BSA (bovine serum albumin)
**All other antibodies were prepared in 5% milk

3.6 Staining for mitochondrial function

Hdh mouse striatal cells were plated onto coverslips coated in a gelatin/fibronectin mixture in a 24-well plate and were then treated with 10μM U0126 for 16 hours in fresh DMEM medium. To determine the effect inhibition of MAPK1 has on mitochondrial membrane potential, striatal cells were incubated with 0.25μM tetramethylrhodamine (TMRM, Invitrogen) for 20 minutes at 33°C. To determine the effect inhibition of MAPK1 has on mitochondrial superoxide production (MitoROS), striatal cells were incubated with 5μM of the mitochondrial superoxide indicator MitoSox™ (Invitrogen) for ten minutes at 33°C. Cells were washed 3X in 1X PBS, stained with Hoechst nuclear dye for five minutes at room

temperature, washed 3X in 1 PBS. Coverslips were then mounted onto slides, and imaged using a confocal microscope (Olympus, Fluoview FV100). At least 100 cells were analyzed from two independent experiments using NIH ImageJ software. Overall densities, from each confocal image, were divided by the number of cells in that image. Histogram depicts the average density of red fluorescence per cell.

3.7 Immunocytochemistry and analysis of mitochondrial morphology

Hdh mouse striatal cells were plated onto coverslips coated in a gelatin/fibronectin mixture in a 24-well plate and were then treated with 10μM U0126 for 16 hours in fresh DMEM medium. To determine the effect inhibition of MAPK1 has on mitochondrial morphology, cells were washed 3X in 1X PBS and then fixed in 4% formaldehyde for ten minutes at room temperature. Cells were washed 3X in 1X PBS and then permeabilized in 0.1% Triton-X 100 for three minutes at room temperature. Cells were blocked in 1% bovine serum albumin (BSA) in PBS containing 0.05% Triton-X 100 for one hour at room temperature. Cells were incubated in primary antibody, Tom20 (1:500, Santa Cruz), for two hours at room temperature. Cells were washed 3X in 1X PBS and then incubated in FITC-labeled goat anti-rabbit antibody overnight at 4°C. Cells were washed 3X in 1X PBS, coverslips were mounted onto slides, and then imaged using a confocal microscope (Olympus, Fluoview FV100). At least 100 cells were analyzed from two independent studies. The percent of fragmented mitochondria was calculated by the number of cells with fragmented mitochondria in an image divided by the total number of cells

in that image. A cell was considered to have fragmented mitochondria if there was a high perinuclear density of mitochondria with a lower amount of mitochondria in the processes of the neurons.

3.8 Transfection of striatal cells with Drp1 S616A mutant

Mutant HdhQ111 mouse striatal cells were plated onto coverslips coated in a gelatin/fibronectin mixture in a 24-well plate. For the transfection mixture 100µL/well of Gibco™ opti-minimum essential medium (MEM, Life Technologies) was incubated with 0.5µL/well of either a control myc vector, or the Drp1 S616A-myc vector, and 1.5µL/well of the transfection reagent *Trans*IT 2020 (Mirus) for 15 minutes at room temperature. Then 100µL of this mixture was added per well and incubated at 33°C, humidified at 5% CO_2 for 26 hours. Then one set of HdhQ111 striatal cells transfected with Drp1 S616A-myc were also treated with 10µM U0126 for 16 hours in fresh DMEM medium. All cells were then probed with anti-Tom20 (Santa Cruz) and anti-myc (Santa Cruz) to determine mitochondrial morphology and which cells were the transfected cells, respectively. Cells were analyzed by confocal microscopy. *Rhodamine-labeled goat anti-rabbit secondary antibody was used for Tom20 and FITC-labeled goat anti-mouse secondary antibody was used for myc.

3.9 Measurement of cell viability

Hdh mouse striatal cells were serum depleted for 8 hours, followed by treatment with 10/25/50μM U0126 for 16 hours in fresh DMEM medium minus serum (for a total of 24 hours of serum starvation). Medium was collected and centrifuged at 400g for ten minutes at 4°C. Cells were lysed in total lysis buffer (10mM HEPES-NaOH pH 7.8, containing 150mM NaCl, 1mM EGTA, 1% Triton X-100, protease inhibitor, and phosphatase inhibitor). The supernatant was collected as lactate dehydrogenase (LDH) in the medium and the lysate was added to the pelleted cells and centrifuged again at 400g for ten minutes at 4°C. Supernatant was collected as LDH in the cells. Supernatants were diluted (10X for medium, and 50X for cells) before 100μL dilated supernatant was added to 100μL reaction solution (Cytotoxicity Detection Kit (LDH), Roche). Reaction was allowed to take place for 30 minutes at room temperature in the dark. Reaction was stopped with 50μL 1M HCl and then measured at 492nm using a microplate reader. Cell death was measured as absorbance from medium/(absorbance from medium + absorbance from cells).

3.10 Statistical analysis

All data was analyzed using NIH ImageJ software. Results are expressed as mean ± SEM. Unpaired Student's *t*-test were used for differences between two groups to assess significance ($p<0.05$), as indicated in the graphs.

CHAPTER IV: FUTURE DIRECTION

4.1 Additional experiments

It was noted that inhibition of MAPK1 decreased the green fluorescence in mutant HdhQ111 striatal cells (**Figure 12**) when probed for Tom20, a component of a translocase in the outer mitochondrial membrane. To determine whether inhibition of MAPK1 decreases the expression of Tom20, total lysates will be harvested from the Hdh striatal cells after 16-hour 10μM U0126 treatment. The proteins in the lysate will be separated by SDS-PAGE and the nitrocellulose membrane will be probed with anti-Tom20. This result will either confirm the decrease in mitochondrial fragmentation seen in mutant HdhQ111 striatal cells after U0126 treatment or give insight into a possible side effect of inhibition of MAPK1 in HD.

To further test the effects of MAPK1's role in the pathogenesis of HD the effect U0126 has on neuronal cell death will be revisited (**Figure 15**). The working concentration for U0126 is 10-50μM for 3-24 hours. U0126 has been shown to have a protective role on mitochondrial fragmentation and dysfunction in HD at a working concentration of 10μM for 16 hours (**Figures 12-14**). As mentioned previously, one adjustment to the protocol would be to treat the striatal cells prior to inducing cell death with serum starvation. This will determine if the inhibitor has

the ability to increase the mitochondria's capacity to handle stress. The U0126 treatment can be increased up to 24 hours with the same dose dependent (10/25/50μM) LDH study as previously described. Yet another possibility would be to look at neuronal survival, using the *in vitro* toxicology assay MTT (Sigma) that determines the cellular metabolic activity, reflecting the number of viable cells present. LDH may not be the most appropriate assay for cell death caused by mitochondrial-induced apoptosis, which is normally a controlled cell death of autodigestion, and releases very little lactate dehydrogenase.

To determine the role phosphorylation of Ser616 of Drp1 has on mitochondrial fragmentation in HD the effect the phosphorylation-deficient mutant of Drp1 has on mitochondrial fragmentation will be revisited. One possibility, already mentioned earlier, would be to use Drp1 KO MEF cells to guarantee that only Drp1-S616A mutant is being expressed. The drawback to this model is that Drp1 KO MEF cells are not considered a model for HD and all it would prove is that Ser616 phosphorylation of Drp1 activates its GTPase activity causing mitochondrial fission. The best approach, even with combined low efficiency of siRNA and transfection, would be to reduce endogenous Drp1 in Hdh striatal cells to improve the probability that the mitochondrial morphology observed is due to the phosphorylation-deficient mutant, S616A, of Drp1. This would be a more accurate confirmation that Ser616 is phosphorylated in HD and plays a role in the pathogenesis of the mitochondrial fragmentation and dysfunction observed in HD.

4.2 The mechanism underlying Drp1 activation by MAPK1 in HD

Phosphorylation of Drp1 by kinases can modify its GTPase activity, its cellular location, and its oligomerization. Phosphorylation at different serine/threonine sites by different kinases has different outcomes on the activity of the GTPase of Drp1. Drp1 is a cytosolic protein that requires activation to translocate to the mitochondria when fission is required. And oligomerization of Drp1 at constriction sites on the outer mitochondrial membrane is required for GTP hydrolysis. MAPK1 has been shown to play no role in the formation of Drp1 tetramer in HD (**Figure 11**). Interestingly, it has been shown that Drp1 is expressed less in the mitochondrial fraction in mutant STQ111 striatal cells compared to wild-type STQ7 striatal cells, with no change seen in mutant HdhQ111 striatal cells compared to wild-type HdhQ7.[64] The main finding in Cherubini et al. 2015 is that the GTPase activity of Drp1 is increased in mutant Q111 striatal cells compared to wild-type Q7, and this is the reason for the increased mitochondrial fission and fragmentation seen in HD.[64]

In order to determine how MAPK1 phosphorylation of Drp1 at Ser616 activates the fission protein the following two experiments should be done. First, to determine if MAPK1 plays a role in the translocation of Drp1 to the mitochondria, Hdh striatal cells will be treated with 10μM U0126 for four hours. Then, using subcellular fractionation, mitochondrial and cytosolic fractions will be obtained.

Samples will be separated by 10% SDS-PAGE, the protein will be transferred to a nitrocellulose membrane, and then the membrane will be probed using anti-Drp1. To determine if the phosphorylation of Drp1 at Ser616 by MAPK1 increases its GTPase activity Hdh striatal cells will be treated with 10μM U0126 for four hours. Total lysates will be harvested from Hdh striatal cells and then incubated with anti-Drp1 followed by A/G beads. The immunoprecipitates will be washed and then the GTPase activity will be determined using a GTPase assay kit. One drawback to the GTPase assay kit being performed on total lysates from cell culture is that immunoprecipitation of Drp1 can pull down other GTPases. Alternatively, this experiment can be performed with recombinant Drp1 and recombinant MAPK1 using an *in vitro* GTPase assay.

4.3 Additional HD models

All experiments performed thus far have been with *in vitro* cell culture models of HD. Taking striatal cells outside of the body's natural environment does not mimic to the best ability a disease state. *In vivo* mouse models can be used to validate that results found *in vitro* properly demonstrate cellular mechanisms of the disease. The first HD mouse model used in preclinical trials is the R6/2 mouse expressing the N-terminal fragment of human mtHtt.[65] This model shows a more aggressive form of HD, showing symptoms at six weeks and living for approximately 15 weeks. Another HD mouse model is the YAC128 mouse expressing full-length

mtHtt.[66] This model has a slower progression of the disease, which better mimics the human condition. YAC128 mice show motor symptoms at the age of six months, neurodegeneration at the age of 12 months and live as long as wild-type mice (2-2.5 years). A drawback to using the mice models is the time required waiting for the mice to grow and start showing symptoms before U0126 treatment can be administered.

Both the Hdh striatal cells and *in vivo* models mentioned above are mice models, which could lead to trouble translating the results observed to the human condition. Two *in vitro* human cell cultures can be used to confirm that the involvement of Drp1 and MAPK1 in mitochondrial fragmentation and dysfunction seen in our models of HD also occurs in the human condition. HeLa human epithelial cells were derived from cervical carcinoma cells and have been previously described.[63] The HeLa cells have been transfected with myc-tagged plasmids containing either 23-polyglutamine repeats (Q23, wild-type) or 73-polyglutamine repeats (Q73, HD). One additional benefit to using this model, apart from it being a human cell line, is it tests the molecular mechanism of the disease in a non-neuronal type of cell. Since mtHtt is ubiquitously expressed in all cell types, showing similar results in epithelial cells will help us better understand why striatal cells are more vulnerable to the effects mtHtt has on the cell. A drawback to using HeLa epithelial cells transfected with mtHtt is that problems can occur where the cells no longer stably express the plasmids.

To validate the results in the context of HD patient genotype, neuronal cells

derived from HD patient-iPS cells[60] should be used as a preclinical model. These HD patient-iPS cells take two months to fully differentiate into neuronal cells. However, even with the time commitment, these cells can be used to validate Ser616 phosphorylation of Drp1, the effects of MAPK1 on cell signaling, mitochondrial fragmentation, mitochondrial dysfunction, and neuronal cell death in HD. Testing the validity of experimental findings in neurons derived from HD patient-iPS cells, before moving to human clinical trials, is not only time and money efficient, but also an ethical step that should be incorporated as a bridge between the scientific method and clinical trials.

4.4 MAPK1 and mutant huntingtin

Since MAPK1 has many diverse cellular effects, inhibition of MAPK1 is not a feasible option for treatment of HD. Therefore, it is important to look upstream of MAPK1 phosphorylation of Drp1 and link MAPK1 to mtHtt (**Figure 19**). The activation of MAPK1 by mtHtt can be either direct or indirect. It has been shown that mtHtt directly binds to Drp1 increasing its GTPase activity.[61] This interaction between mtHtt and Drp1 can make the fission protein more susceptible to phosphorylation by MAPK1. As discussed earlier, mutant huntingtin N-terminal fragments can enter the nucleus and alter gene transcription.[22] This altered gene transcription can lead to over-activation of the MAP kinase signaling pathway.

To investigate the connection between mtHtt and mitochondrial dysfunction activated by MAPK1 seen in our models of HD, a first step would be to analyze the

interactome for mtHtt compared to wild-type Htt. This will give some indication to what molecular and cellular functions in the cell have been given a toxic gain-of-function by mtHtt. This will help determine if mtHtt has a direct or indirect effect on the activation of MAPK1 and Drp1 in the mitochondrial dysfunction seen in HD. Next, co-immunoprecipitation can be performed to determine if there is an increased interaction with mtHtt and any mitochondrial proteins, kinases/phosphatases, or transcriptional factors in HD. After determining an interaction, inhibiting it and observing the effect it has on mitochondrial morphology and function would demonstrate mtHtt plays a role in the activation of mitochondrial fragmentation and dysfunction seen in HD.

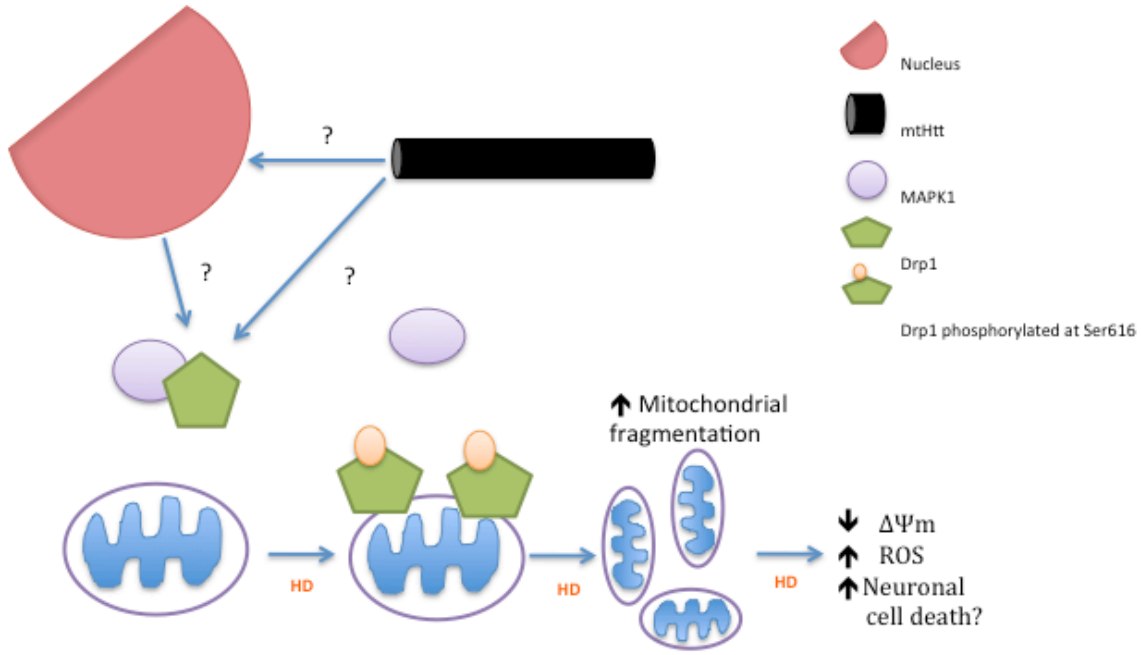

Figure 19. The role mtHtt plays in MAPK1 and Drp1 activation in HD. mtHtt can directly activate Drp1 and/or MAPK1 or mtHtt can indirectly activate this process by altering transcription.

*not to scale

APPENDIX I: SUPPLEMENTAL FIGURES- CHROMATOGRAMS & SPECTRA

Figure A1. HPLC chromatogram of trypsin digest of Drp1 phosphorylated by MAPK1.

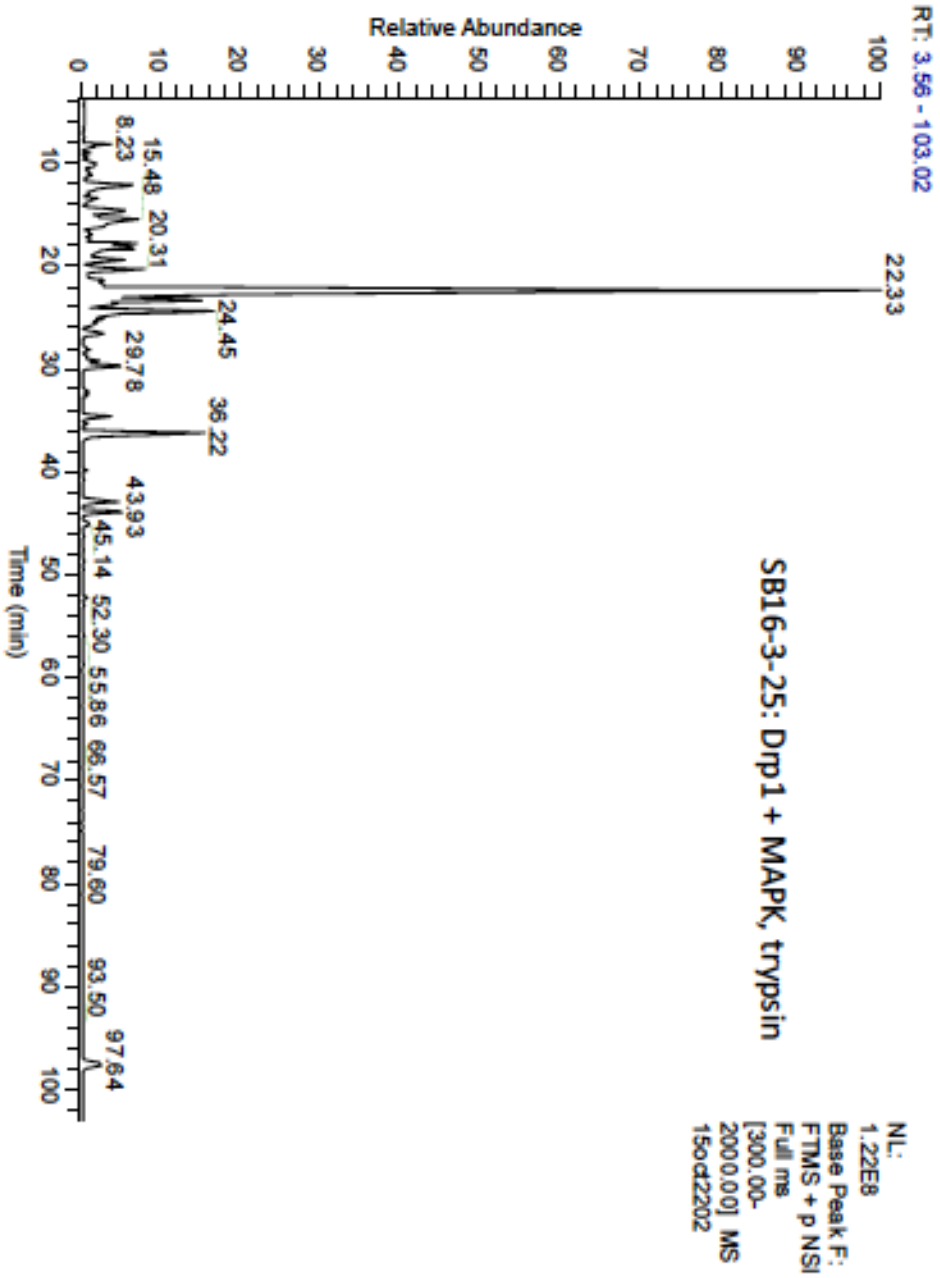

Figure A2. HPLC chromatogram of chymotrypsin digest of Drp1 phosphorylated by MAPK1.

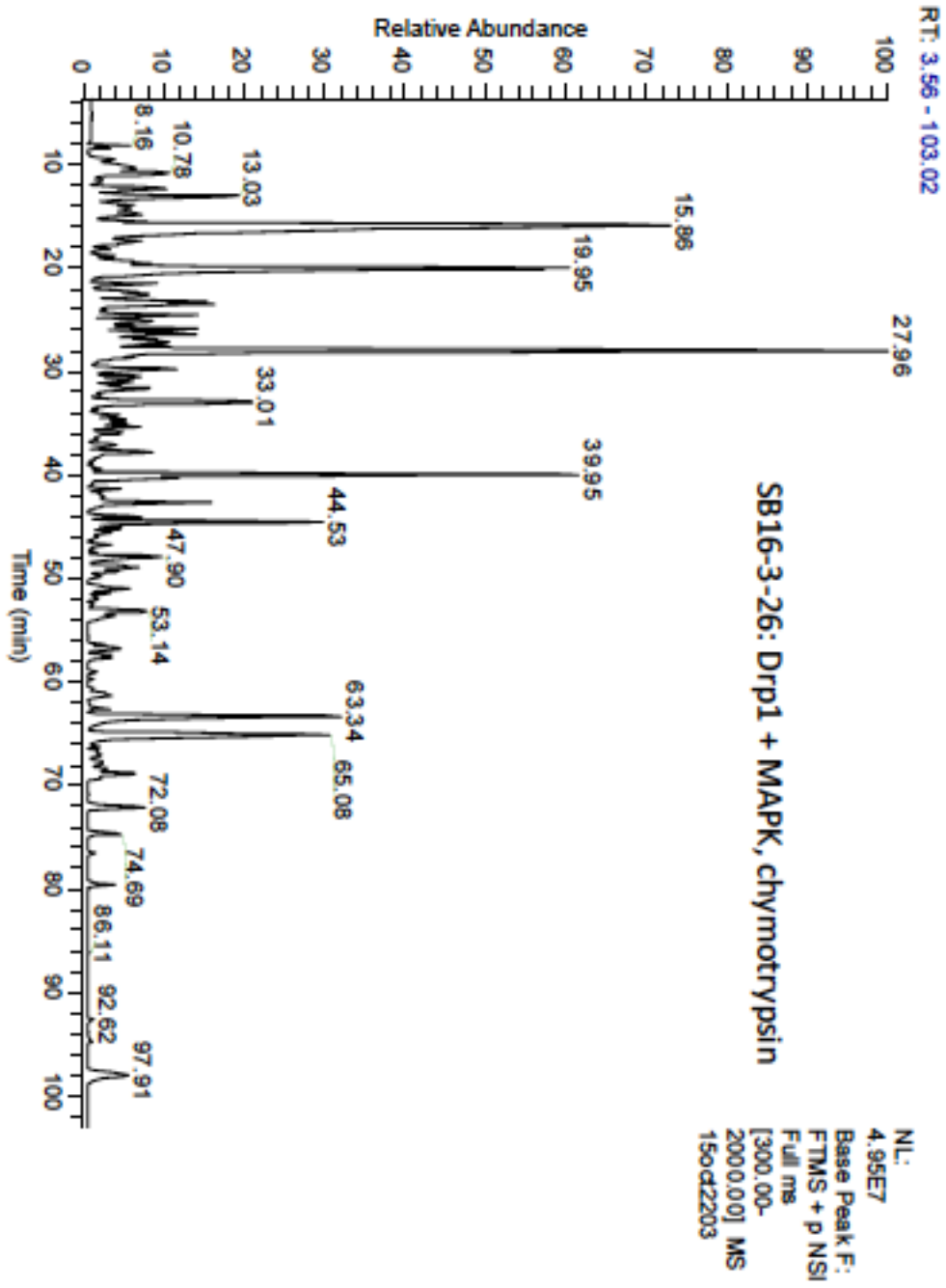

Figure A3. CID mass spectrum of phosphopeptide identifying S126. Drp1 isoform 2.

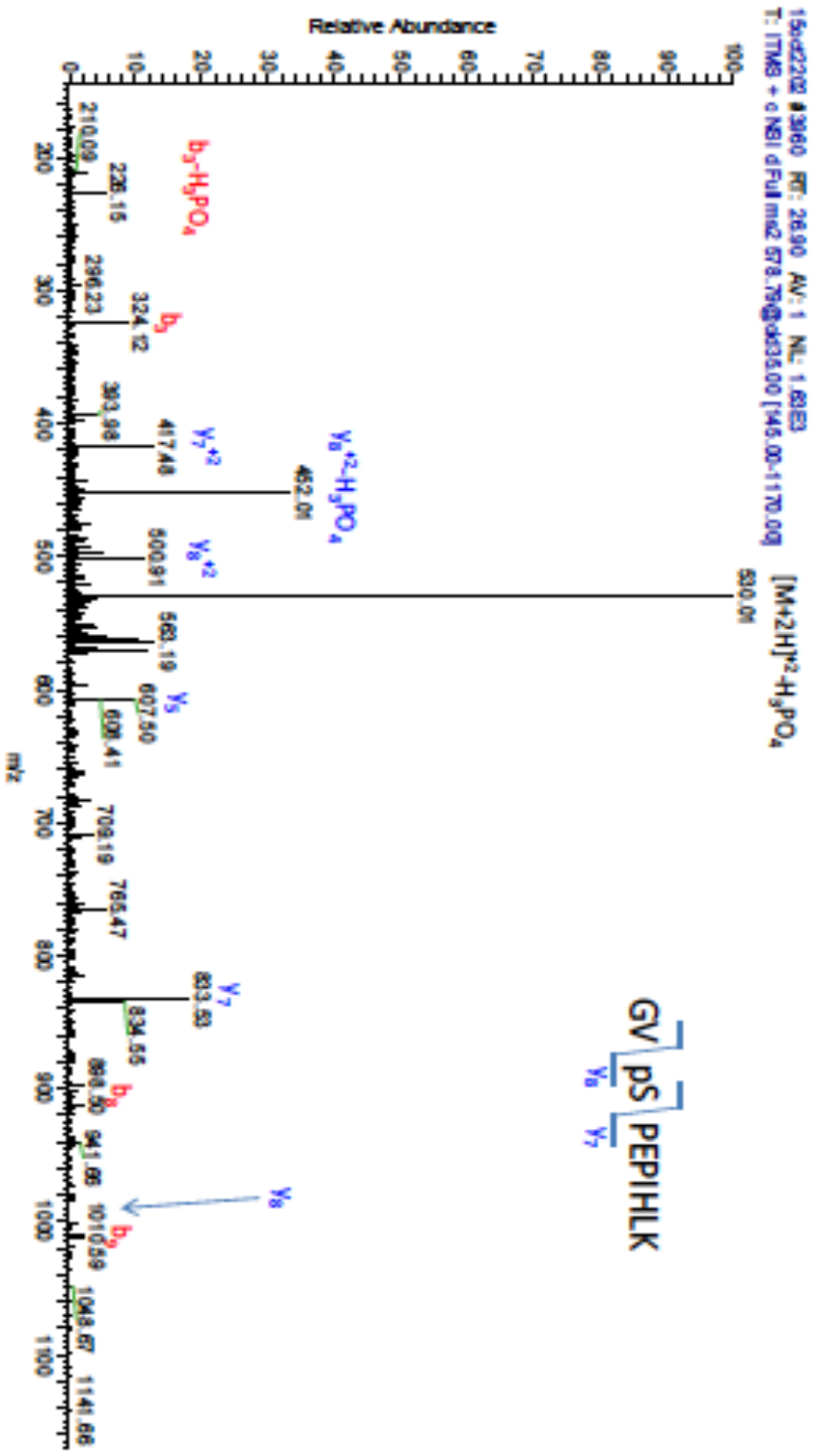

Figure A4. CID mass spectrum of phosphopeptide identifying S248. Drp1 isoform 2.

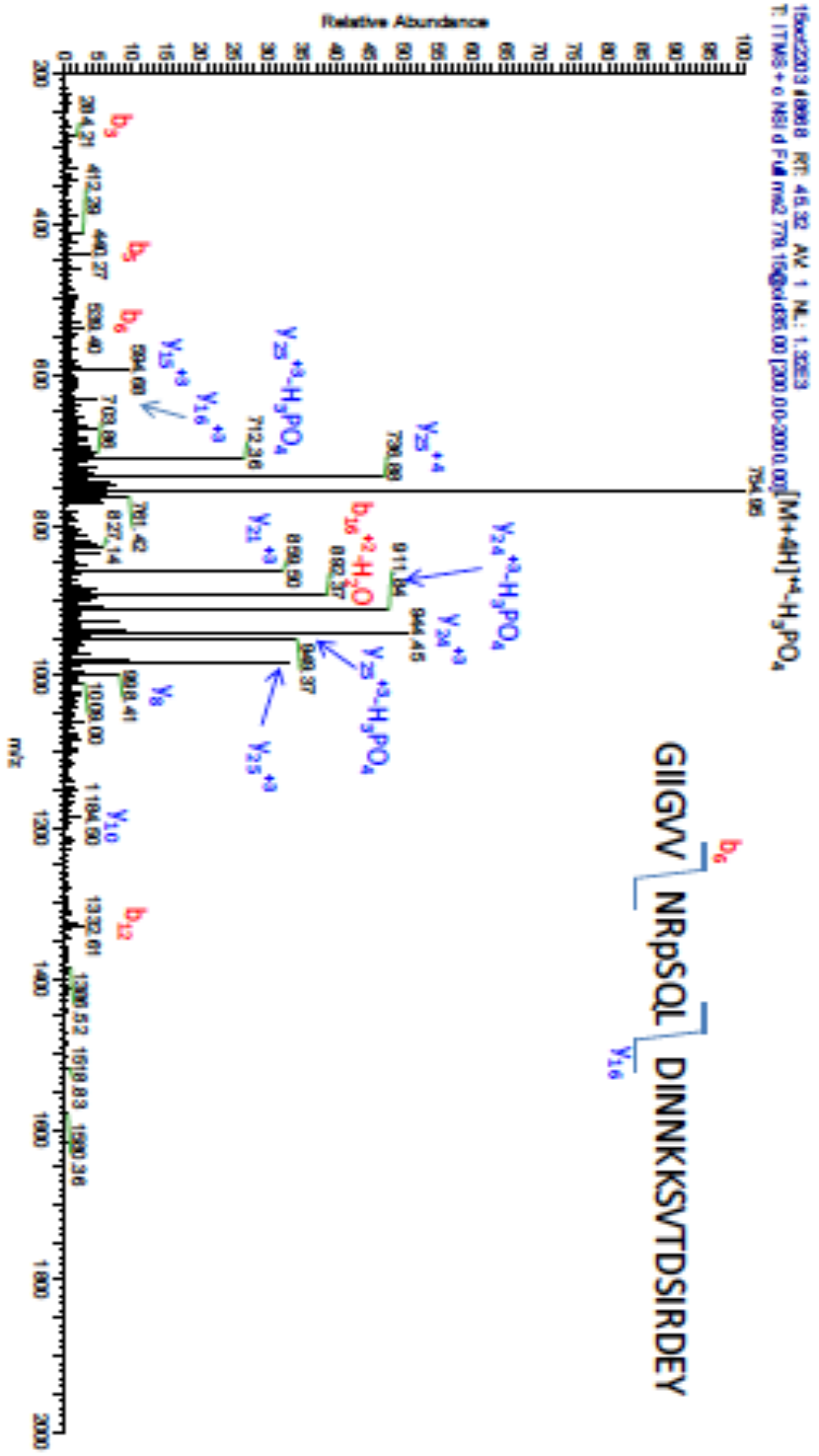

Figure A5. CID mass spectrum of phosphopeptide identifying S275. Drp1 isoform 2.

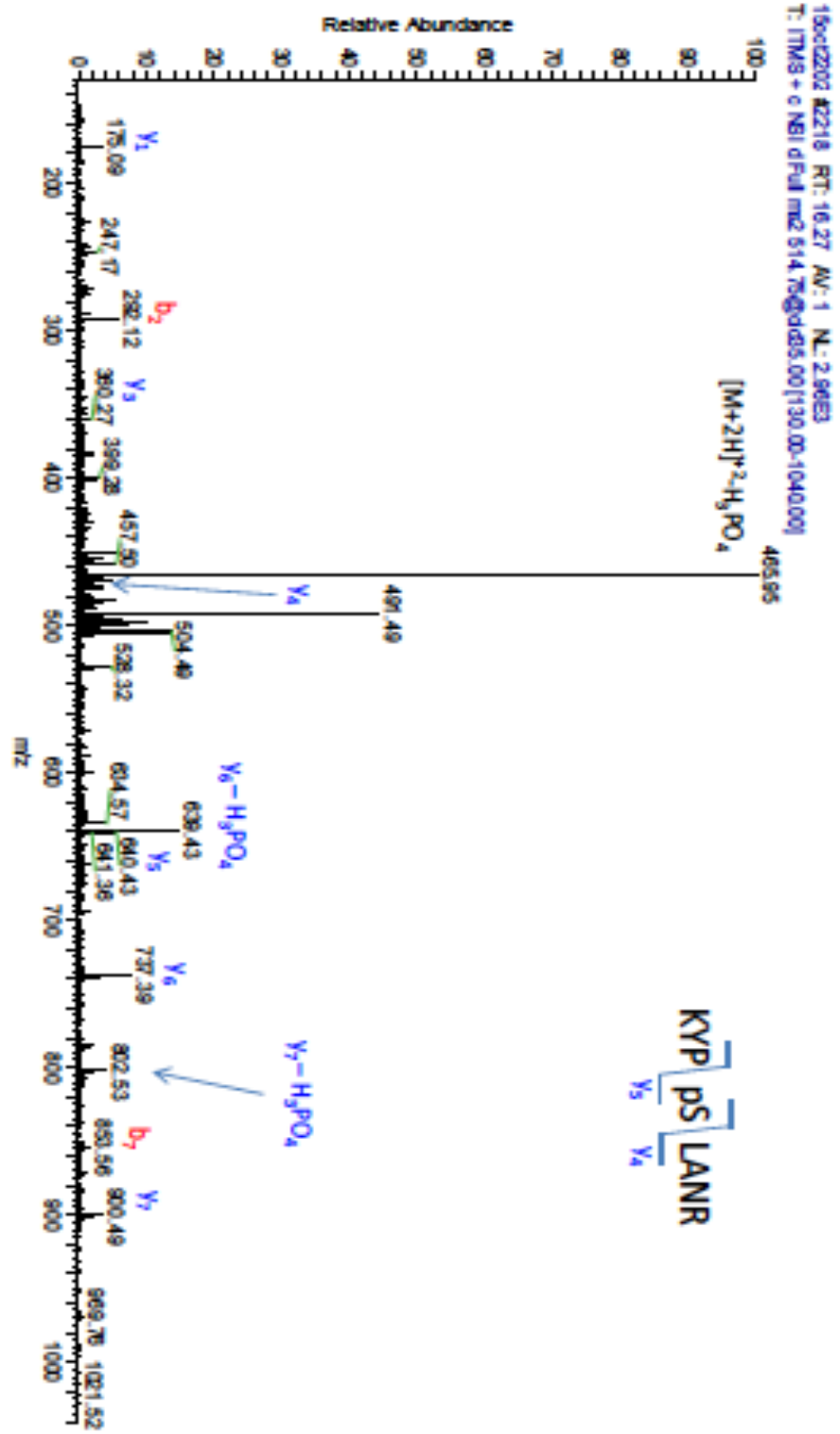

Figure A6. CID mass spectrum of phosphopeptide identifying S529. Drp1 isoform 2.

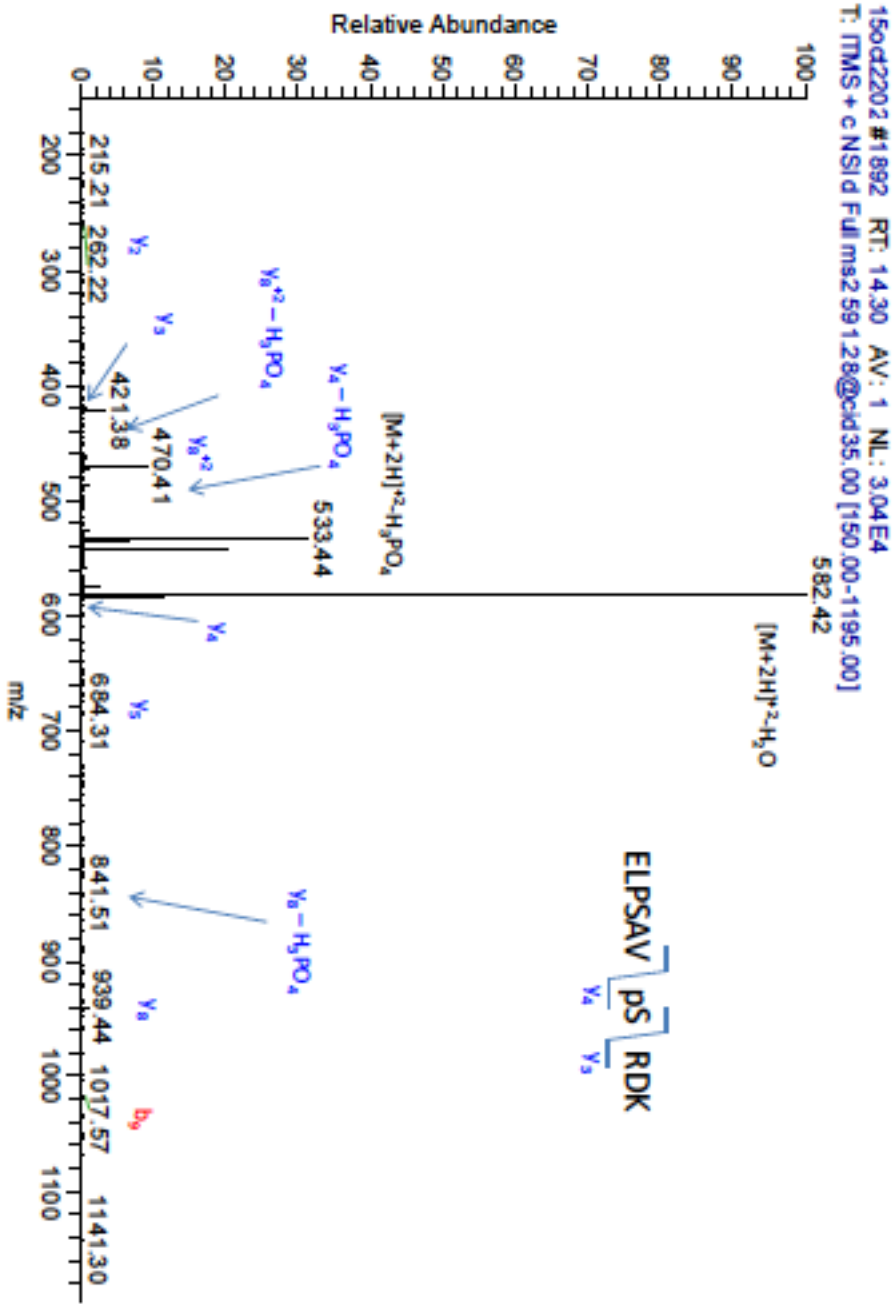

Figure A7. CID mass spectrum of phosphopeptide identifying S590. Drp1 isoform 2.

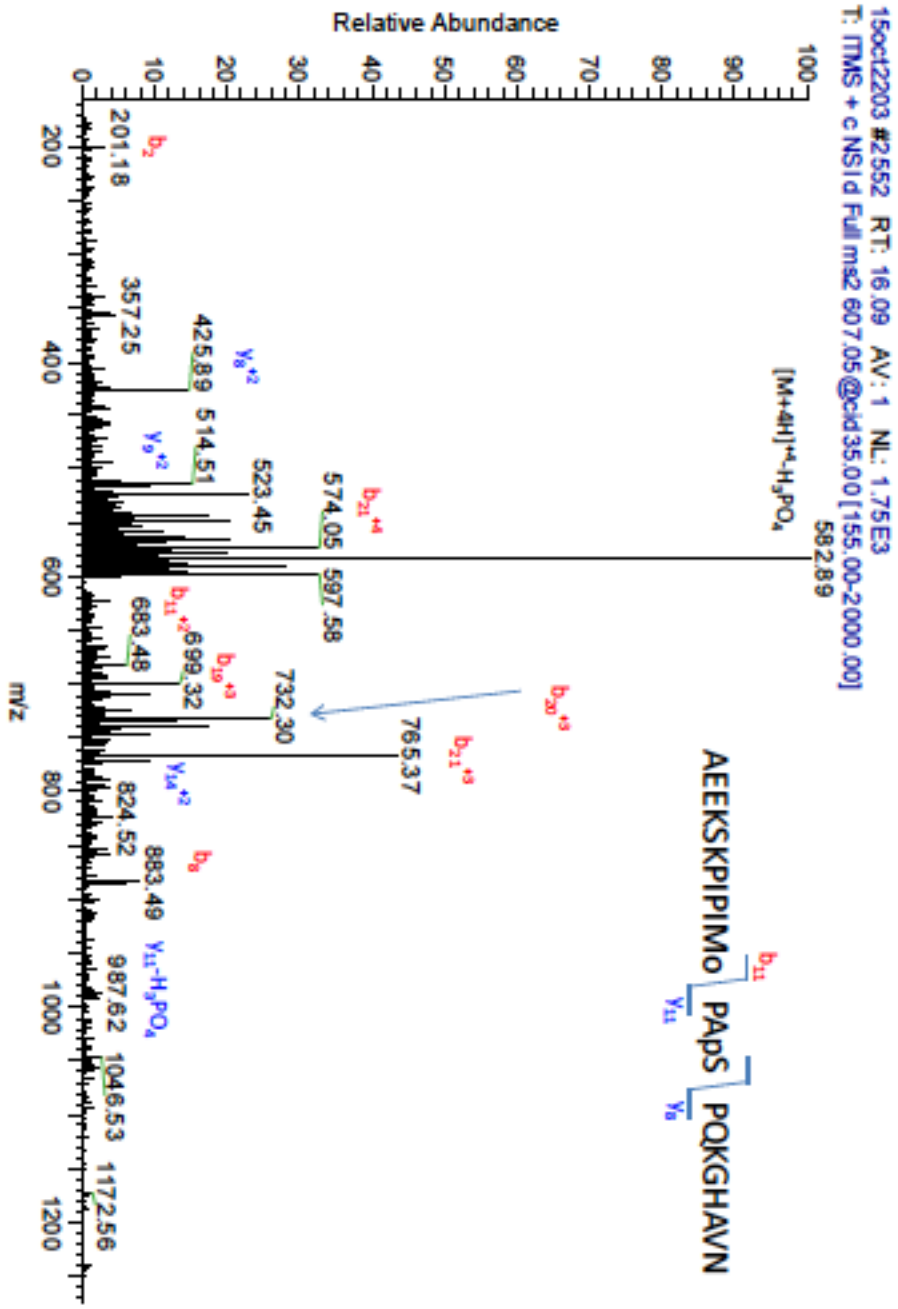

Figure A8. CID mass spectrum of phosphopeptide identifying S611. Drp1 isoform 2.

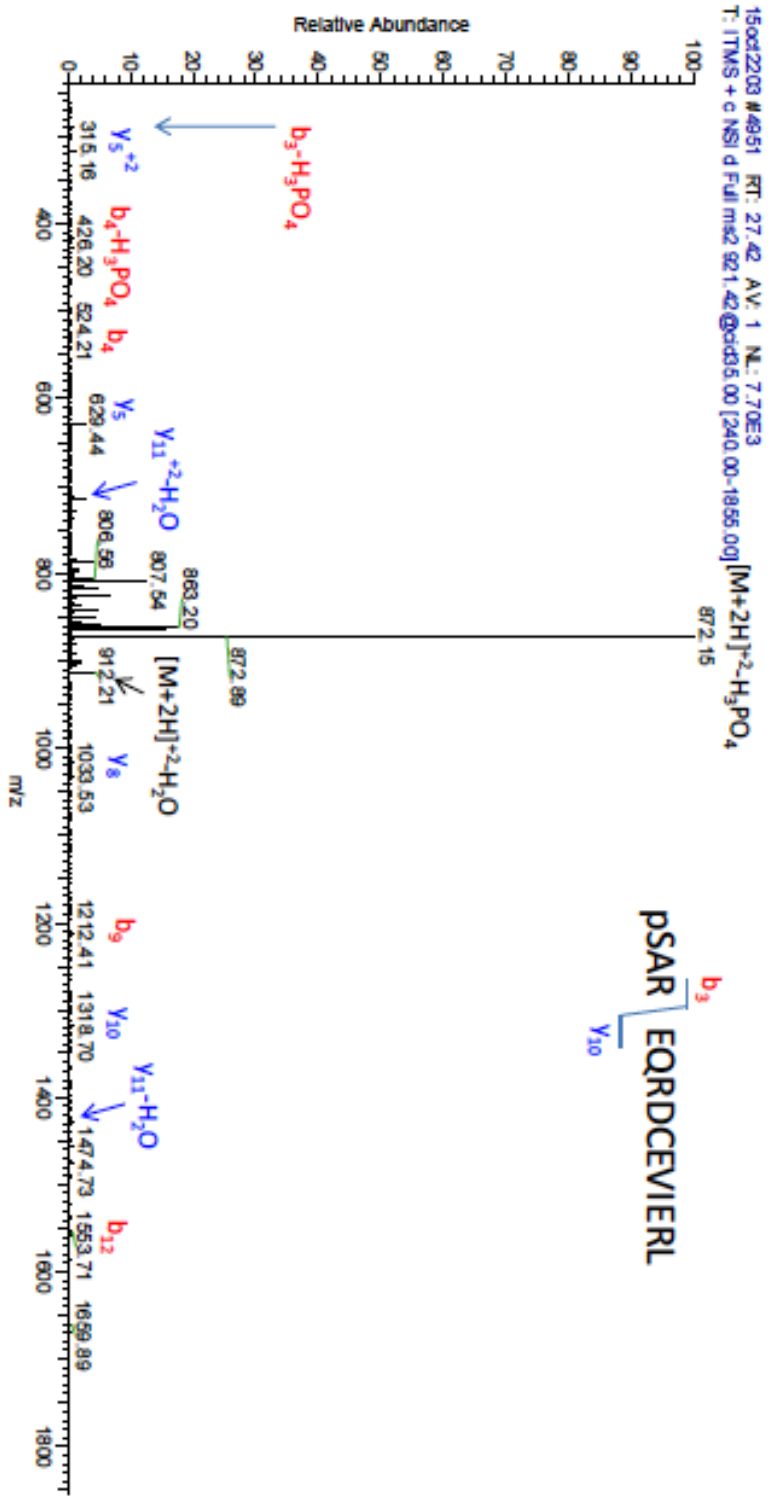

REFERENCES

1. Pringsheim T, Wiltshire K, Day L, Dykeman J, Steeves T, Jette N (2012). The incidence and prevalence of huntington's disease: A systematic review and meta-analysis. Movement Disorders 27: 1083-1091.

2. Huntington G (1872). On Chorea. In Medical and Surgical Reporter 26: 320–321, Philadelphia.

3. Water CO (1842). In Practice of Medicine 2: 312. (R. Dunglison, ed.), Lee and Blanchard, Philadelphia.

4. Meynert T (1877). Discussion to Fritsch. Psychiatry 4: 47.

5. The Huntington's Disease Collaborative Research Group (1993). A novel gene containing a trinucleotide repeat that is expanded and unstable on Huntington's disease chromosomes. Cell 72: 971–983.

6. Ross CA (1995). When more is less: pathogenesis of glutamine repeat neurodegenerative diseases. Neuron 15: 493–496.

7. Perutz MF (1999). Glutamine repeats and neurodegenerative diseases: molecular aspects. Trends Biochem. Sci. 24: 58–63.

8. Ordway JM, Tallaksen-Greene S, Gutekunst CA, Bernstein EM, Cearley JA, Wiener HW, Dure 4th LS, Lindsey R, Hersch SM, Jope RS, Albin RL, Detloff PJ (1997). Ectopically expressed CAG repeats cause intranuclear inclusions and a progressive late onset neurological phenotype in the mouse. Cell 91: 753–763.

9. Marsh JL, Walker H, Theisen H, Zhu YZ, Fielder T, Purcell J, Thompson LM (2000). Expanded polyglutamine peptides alone are intrinsically cytotoxic and cause neurodegeneration in Drosophila. Hum. Mol. Genet. 9: 13–25.

10. Rockabrand E, Slepko N, Pantalone A, Nukala VN, Kazantsev A, Marsh JL, Sullivan PG, Steffan JS, Sensi SL, Thompson LM (2007). The first 17 amino acids of huntingtin modulate its sub-cellular localization, aggregation and effects on calcium homeostasis. Hum. Mol. Genet. 16: 61–77.

11. Atwal RS, Xia J, Pinchev D, Taylor J, Epand RM, Truant R (2007). Huntingtin has a membrane association signal that can modulate huntingtin aggregation, nuclear entry and toxicity. Hum. Mol. Genet. 16: 2600–2615.

12. Nasir J, Floresco SB, O'Kusky JR, Diewert VM, Richman JM, Zeisler J, Borowski A, Marth JD, Phillips AG, Hayden MR (1995). Targeted disruption of the Huntington's disease gene results in embryonic lethality and behavioral and morphological changes in heterozygotes. Cell 81: 811–823.

13. Zeitlin S, Liu JP, Chapman DL, Papaioannou VE, Efstratiadis A (1995). Increased apoptosis and early embryonic lethality in mice nullizygous for the Huntington's disease gene homologue. Nat. Genet. 11: 155–163.

14. Dragatsis I, Levine MS, Zeitlin S (2000). Inactivation of Hdh in the brain and testis results in progressive neurodegeneration and sterility in mice. Nat. Genet. 26: 300–306.

15. Rigamonti D, Sipione S, Goffredo D, Zuccato C, Fossale E, Cattaneo E (2001). Huntingtin's neuroprotective activity occurs via inhibition of procaspase-9 processing. J. Biol. Chem. 276: 14545–14548.

16. Ho LW, Brown R, Maxwell M, Wyttenbach A, Rubinsztein DC (2001). Wild type huntingtin reduces the cellular toxicity of mutant huntingtin in mammalian cell models of Huntington's disease. J. Med. Genet. 38: 450–452.

17. Rigamonti D, Bauer JH, De-Fraja C, Conti L, Sipione S, Sciorati C, Clementi E, Hackam A, Hayden MR, Li Y, Cooper JK, Ross CA, Govoni S, Vincenz C, Cattaneo E (2000). Wild-type huntingtin protects from apoptosis upstream of caspase-3. J. Neurosci. 20: 3705–3713.

18. Gafni J, Hermel E, Young JE, Wellington CL, Hayden MR, Ellerby LM (2004). Inhibition of calpain cleavage of huntingtin reduces toxicity: accumulation of

calpain/caspase fragments in the nucleus. J. Biol. Chem. 279: 20211–20220.

19. Graham RK, Deng Y, Slow EJ, Haigh B, Bissada N, Lu G, Pearson J, Shehadeh J, Bertram L, Murphy Z, Warby SC, Doty CN, Roy S, Wellington CL, Leavitt BR, Raymond LA, Nicholson DW, Hayden MR (2006). Cleavage at the caspase-6 site is required for neuronal dysfunction and degeneration due to mutant huntingtin. Cell 125: 1179–1191.

20. Saudou F, Finkbeiner S, Devys D, Greenberg ME (1998). Huntingtin acts in the nucleus to induce apoptosis but death does not correlate with the formation of intranuclear inclusions. Cell 95: 55–66.

21. Schilling G, Savonenko AV, Klevytska A, Morton JL, Tucker SM, Poirier M, Gale A, Chan N, Gonzales V, Slunt HH (2004). Nuclear-targeting of mutant huntingtin fragments produces Huntington's disease-like phenotypes in transgenic mice. Hum. Mol. Genet. 13: 1599–1610.

22. Gerber HP, Seipel K, Georgiev O, Hofferer M, Hug M, Rusconi S, Schaffner W (1994). Transcriptional activation modulated by homopolymeric glutamine and proline stretches. Science 263: 808–811.

23. Hackam AS, Singaraja R, Wellington CL, Metzler M, McCutcheon K, Zhang T, Kalchman M, Hayden MR (1998). The influence of huntingtin protein size on nuclear

localization and cellular toxicity. J. Cell Biol. 141: 1097–1105.

24. Wyttenbach A, Carmichael J, Swartz J, Furlong RA, Narain Y, Rankin J, Rubinsztein DC (2000). Effects of heat shock, heat shock protein 40 (HDJ-2), and proteasome inhibition on protein aggregation in cellular models of Huntington's disease. Proc. Natl. Acad. Sci. U.S.A. 97: 2898–2903.

25. Bodner RA, Outeiro TF, Altmann S, Maxwell MM, Cho SH, Hyman BT, McLean PJ, Young AB, Housman DE, Kazantsev AG (2006). Pharmacological promotion of inclusion formation: a therapeutic approach for Huntington's and Parkinson's diseases. Proc. Natl. Acad. Sci. U.S.A. 103: 4246–4251.

26. Arrasate M, Mitra S, Schweitzer ES, Segal MR, Finkbeiner S (2004). Inclusion body formation reduces levels of mutant huntingtin and the risk of neuronal death. Nature 431: 805–810.

27. Beal MF (2005). Mitochondria take center stage in aging and neurodegeneration. Ann. Neurol. 58: 495–505.

28. Lin MT, Beal MF (2006). Mitochondrial dysfunction and oxidative stress in neurodegenerative diseases. Nature 443: 787–795.

29. Trushina E, McMurray CT (2007). Oxidative stress and mitochondrial

dysfunction in neurodegenerative diseases. Neuroscience 145: 1233–1248.

30. Chan DC (2006). Mitochondria: dynamic organelles in disease, aging, and development. Cell 125: 1241–1252.

31. Hoppins S, Lackner L, Nunnari J (2007). The machines that divide and fuse mitochondria. Annu Rev Biochem 76: 751–780.

32. Seong IS, Ivanova E, Lee JM, Choo YS, Fossale E, Anderson M, Gusella JF, Laramie JM, Myers RH, Lesort M, MacDonald ME (2005). HD CAG repeat implicates a dominant property of huntingtin in mitochondrial energy metabolism. Hum. Mol. Genet. 14: 2871–2880.

33. Novelli A, Reilly JA, Lysko PG, Henneberry RC (1988). Glutamate becomes neurotoxic via the N-methyl-D-aspartate receptor when intracellular energy levels are reduced. Brain Res. 451: 205–212.

34. Fagni L, Lafon-Cazal M, Rondouin G, Manzoni O, Lerner-Natoli M, Bockaert J (1994). The role of free radicals in NMDA-dependent neurotoxicity. Prog. Brain Res. 103: 381–390.

35. Costa V, Scorrano L (2012). Shaping the role of mitochondria in the pathogenesis of Huntington's disease. EMBO J. 31: 1853–1864.

36. Cui L, Jeong H, Borovecki F, Parkhurst CN, Tanese N, Krainc D (2006). Transcriptional repression of PGC-1alpha by mutant huntingtin leads to mitochondrial dysfunction and neurodegeneration. Cell 127: 59–69.

37. Weydt P, Pineda VV, Torrence AE, Libby RT, Satterfield TF, Lazarowski ER, Gilbert ML, Morton GJ, Bammler TK, Strand AD, Cui L, Beyer RP, Easley CN, Smith AC, Krainc D, Luquet S, Sweet IR, Schwartz MW, La Spada AR (2006). Thermoregulatory and metabolic defects in Huntington's disease transgenic mice implicate PGC-1alpha in Huntington's disease neurodegeneration. Cell Metab 4: 349–362.

38. Chaturvedi RK, Adhihetty P, Shukla S, Hennessy T, Calingasan N, Yang L, Starkov A, Kiaei M, Cannella M, Sassone J, Ciammola A, Squitieri F, Beal MF (2009). Impaired PGC-1alpha function in muscle in Huntington's disease. Hum Mol Genet 18: 3048–3065.

39. Panov AV, Gutekunst CA, Leavitt BR, Hayden MR, Burke JR, Strittmatter WJ, Greenamyre JT (2002). Early mitochondrial calcium defects in Huntington's disease are a direct effect of polyglutamines. Nat Neurosci 5: 731–736.

40. Bernardi P, Forte M (2007). The mitochondrial permeability transition pore. Novartis Found Symp 287: 157–164; discussion 164–169.

41. Brennan Jr WA, Bird ED, Aprille JR (1985). Regional mitochondrial respiratory activity in Huntington's disease brain. J Neurochem 44: 1948–1950.

42. Gu M, Gash MT, Mann VM, Javoy-Agid F, Cooper JM, Schapira AH (1996). Mitochondrial defect in Huntington's disease caudate nucleus. Ann Neurol 39: 385–389.

43. Bossy-Wetzel E, Petrilli A, Knott AB (2008). Mutant Huntingtin and mitochondrial dysfunction. Trends Neurosci 31: 609–616.

44. Benard G, Rossignol R (2008). Ultrastructure of the mitochondrion and its bearing on function and bioenergetics. Antioxid Redox Signal 10: 1313–1342.

45. Yu T, Robotham JL, Yoon Y (2006). Increased production of reactive oxygen species in hyperglycemic conditions requires dynamic change of mitochondrial morphology. Proc Natl Acad Sci USA 103: 2653–2658.

46. Li Z, Okamoto K, Hayashi Y, Sheng M (2004). The importance of dendritic mitochondria in the morphogenesis and plasticity of spines and synapses. Cell 119: 873–887.

47. Wasilewski M, Scorrano L (2009). The changing shape of mitochondrial

apoptosis. Trends Endocrinol Metab 20: 287–294.

48. Frank S, Gaume B, Bergmann-Leitner ES, Leitner WW, Robert EG, Catez F, Smith CL, Youle RJ (2001). The role of dynamin-related protein 1, a mediator of mitochondrial fission, in apoptosis. Dev Cell 1: 515–525.

49. Scorrano L, Ashiya M, Buttle K, Weiler S, Oakes SA, Mannella CA, Korsmeyer SJ (2002). A distinct pathway remodels mitochondrial cristae and mobilizes cytochrome c during apoptosis. Dev Cell 2: 55–67.

50. Germain M, Mathai JP, McBride HM, Shore GC (2005). Endoplasmic reticulum BIK initiates DRP1-regulated remodelling of mitochondrial cristae during apoptosis. EMBO J 24: 1546–1556.

51. Qi X, Disatnik MH, Shen N, Sobel RA, Mochly-Rosen D (2011). Aberrant mitochondrial fission in neurons induced by protein kinase C{delta} under oxidative stress conditions in vivo. Mol Biol Cell 22: 256-265.

52. Baloh RH, Schmidt RE, Pestronk A, Milbrandt J (2007). Altered axonal mitochondrial transport in the pathogenesis of Charcot-Marie-Tooth disease from mitofusin 2 mutations. J Neurosci 27: 422–430.

53. Taguchi N, Ishihara N, Jofuku A, Oka T, Mihara K (2007). Mitotic phosphorylation of dynamin-related GTPase Drp1 participates in mitochondrial fission. J. Biol. Chem. 282: 11521–11529.

54. Chang CR, Blackstone C (2007). Cyclic AMP-dependent protein kinase phosphorylation of Drp1 regulates its GTPase activity and mitochondrial morphology. J Biol Chem 282: 21583-21587.

55. Cribbs JT, Strack S (2007). Reversible phosphorylation of Drp1 by cyclic AMP dependent protein kinase and calcineurin regulates mitochondrial fission and cell death. EMBO Rep 8: 939-944.

56. Su YC, Qi X (2013). Inhibition of excessive mitochondrial fission reduced aberrant autophagy and neuronal damage caused by LRRK2 G2019S mutation. Hum Mol Genet. 22: 4545-4561.

57. Pyakurel A, Savoia C, Hess D, Scorrano L (2015). Extracellular regulated kinase phosphorylates mitofusin 1 to control mitochondrial morphology and apoptosis. Molecular Cell 58: 244-254.

58. Serasinghe MN, Wieder SY, Kenault TT, Elkholi R, Asciolla JJ, Yao JL, Jabado O, Hoehnk K, Kageyama Y, Sesaki H, Chipuk JE (2015). Mitochondrial division is

requisite to RAS-induced transformation and targeted by oncogenic MAPK pathway inhibitors. Molecular Cell 57: 521-536.

59. Kashatus JA, Nascimento A, Myers LJ, Sher A, Byrne FL, Hoehn KL, Counter CM, Kashatus DF (2015). Erk2 phosphorylation of Drp1 promotes mitochondrial fission and MAPK-driven tumor growth. Molecular Cell 57: 537-551.

60. Guo X, Disatnik MH, Monbureau M, Shamloo M, Mochly-Rosen D, Qi X (2013). Inhibition of mitochondrial fragmentation diminishes Huntington's disease–associated neurodegeneration. Journal of Clinical Investigation 123: 5371-5388.

61. Song W, Chen J, Petrilli A, Liot G, Klinglmayr E, Zhou Y, Poquiz P, Tjong J, Pouladi M.A, Hayden M.R, Masliah E, Ellisman M, Rouiller I, Schwarzenbacher R, Bossy B, Perkins G, Bossy-Wetzel E (2011). Mutant huntingtin binds the mitochondrial fission GTPase dynamin-related protein-1 and increases its enzymatic activity. Nat Med 17:377-382.

62. Trettel F, Rigamonti D, Hilditch-Maguire P, Wheeler VC, Sharp AH, Persichetti F, Cattaneo E, MacDonald ME (2000). Dominant phenotypes produced by the HD mutation in STHdh(Q111) striatal cells. Human Molecular Genetics 9: 2799-2809.

63. Gey GO, Coffman WD, Kubicek MT (1952). Tissue culture studies of the proliferative capacity of cervical carcinoma and normal epithelium. Cancer Res. 12: 264–265.

64. Cherubini M, Puigdellívol, M, Alberch J, Ginés, S (2015). Cdk-5-mediated mitochondrial fission: a key player in dopaminergic toxicity in Hintington's disease.Biochimica et Biophysica Acta. 1852: 2145-2160.

65. Cha JH, Kosinski CM, Kerner JA, Alsdorf SA, Mangiarini L, Davies SW, Penney JB, Bates GP, Young AB (1998). Altered brain neurotransmitter receptors in transgenic mice expressing a portion of an abnormal human Huntington disease gene. Proceedings of the National Academy of Sciences 95: 6480-6485.

66. Slow EJ, van Raamsdonk J, Rogers D, Coleman SH, Graham RK, Deng Y, Oh R, Bissada N, Hossain SM, Yang YZ, Li XJ, Simpson EM, Gutekunst CA, Leavitt BR, Hayden MR (2003). Selective striatal neuronal loss in a YAC128 mouse model of Huntington disease. Human Molecular Genetics 12: 1555-1567.